Commun. Math. Phys. 355, 51–95 (2017)
Digital Object Identifier (DOI) 10.1007/s00220-017-2921-y

Communications in
Mathematical
Physics

# Circular Pentagons and Real Solutions of Painlevé VI Equations

**Alexandre Eremenko, Andrei Gabrielov**

Department of Mathematics, Purdue University, West Lafayette, IN 47907, USA.
E-mail: eremenko@math.purdue.edu

Received: 8 November 2016 / Accepted: 28 April 2017
Published online: 2 June 2017 – © Springer-Verlag Berlin Heidelberg 2017

**Abstract:** We study real solutions of a class of Painlevé VI equations. To each such solution we associate a geometric object, a one-parametric family of circular pentagons. We describe an algorithm that permits to compute the numbers of zeros, poles, 1-points and fixed points of the solution on the interval $(1, +\infty)$ and their mutual position. The monodromy of the associated linear equation and parameters of the Painlevé VI equation are easily recovered from the family of pentagons.

## 0. Introduction

Consider a linear differential equation

$$w'' - Pw' + Qw = 0, \tag{1}$$

where $P$ and $Q$ are rational functions of the complex independent variable, and assume that all singularities are regular, and all parameters (singular points, exponents and accessory parameters) are real. Then the ratio $f = w_1/w_2$ of two linearly independent solutions maps the upper half-plane onto a circular polygon (see Sect. 3 below for a precise definition). Every simply connected circular polygon can be obtained this way. Klein [31] and Van Vleck [44] used this connection between differential equations with three singularities and circular triangles to count zeros and poles of hypergeometric functions. We use a similar idea to count special points on a real interval of real solutions of Painlevé VI equations

$$q_{xx} = \frac{1}{2}\left(\frac{1}{q} + \frac{1}{q-1} + \frac{1}{q-x}\right) q_x^2 - \left(\frac{1}{x} + \frac{1}{x-1} + \frac{1}{q-x}\right) q_x \tag{2}$$
$$+ \frac{q(q-1)(q-x)}{2x^2(x-1)^2}\left\{\kappa_4^2 - \kappa_1^2\frac{x}{q^2} + \kappa_2^2\frac{x-1}{(q-1)^2} + (1-\kappa_3^2)\frac{x(x-1)}{(q-x)^2}\right\},$$

A. Eremenko: Supported by NSF Grant DMS-1665115.
A. Gabrielov: Supported by NSF Grant DMS-1161629.

where $q$ is a function of $x$, and $\kappa_j$ are real parameters. By definition, *special points* of a solution are those points $x$ for which $q(x) \in \{0, 1, x, \infty\}$, the points where the assumptions of the existence and uniqueness theorem of Cauchy are violated.

Equation (2), which we call PVI, was originally discovered by Picard [40], Painlevé [39] and Gambier [19] as the most general equation of the form

$$q_{xx} = R(q_x, q, x), \tag{3}$$

where $R$ is a rational function of $q_x, q$ whose coefficients are analytic in $x$, and whose solutions have no movable singularities (poles are not counted as singularities). For PVI, this means that all solutions admit a meromorphic continuation in the region $\mathbf{C}\backslash\{0, 1\}$. Painlevé and Gambier classified all equations (3) without movable singularities, and found that all except six of them can be reduced to linear or first order differential equations. Of the six remaining equations, PVI is the most general, in the sense that the other five can be obtained from it by certain degeneration process.

Meanwhile, Fuchs [18] independently discovered (2) as the condition of isomonodromic deformation of a linear differential equation (1) with five regular singularities, one of them apparent with exponents 0 and 2. Later it was found that Painlevé equations arise in a variety of problems of mathematics and physics [9,24,32,34], and their solutions, called Painlevé transcendents, gradually gain the status of special functions.

Besides applications, most work on PVI falls into three categories: (a) transformations of the equation [28,37], (b) search for special solutions, like algebraic ones [33] or those expressed in terms of classical special functions [24], and (c) asymptotics at the fixed singularities $0, 1, \infty$ [23,30].

In this paper, we study real solutions of PVI with real parameters $\kappa_j$ on a real interval, one of the three intervals between the fixed singularities $(0, 1, \infty)$. It is sufficient to consider the interval $(1, \infty)$. Our main result is a combinatorial algorithm (which can be performed without a computer) that determines the number of special points and their mutual position on the interval. The outcome of the algorithm is a sequence of symbols $0, 1, x, \infty$ which shows in which order the solution $q(x)$ of (2) takes these four values as $x$ increases from 1 to $\infty$. For example, an outcome sequence $(0, 1, 1, x, \infty)$ means that for the solution $q(x)$ there are points $1 < x_1 < x_2 < x_3 < x_4 < x_5 < +\infty$ such that

$$q(x_1) = 0, \quad q(x_2) = q(x_3) = 1, \quad q(x_4) = x_4, \quad q(x_5) = \infty,$$

and no other special points on $(1, +\infty)$. The sequence of special points can be finite, or infinite in one direction, or infinite in both directions.

In particular, we describe those solutions that have no special points on $(1, \infty)$. Theorem 1 in Sect. 10 implies that

*Every PVI equation with real parameters $\kappa_j$ has a real solution without special points on $(1, +\infty)$. The projective monodromy representation of the auxiliary linear equation (4) corresponding to such a solution satisfies the condition that for some $j \in \{1, \dots, 4\}$ the generators $T_{j-1}$ and $T_j$ share the fixed point where their multipliers are $e^{2\pi i\kappa_{j-1}}$ and $e^{2\pi i\kappa_j}$. For given parameters $\kappa_j$, there can be at most one-dimensional family of such solutions.*

For a more precise formulation, see Sect. 10. This theorem allows us to give new proofs of the recent results in [6,7] for the case of real solutions.

So we obtain global, exact (non-asymptotic) results describing qualitative features of a quite general class of solutions, namely real solutions.

We do this by exploring the connection with a linear differential equation of the type (1) with 5 regular singularities, one of them apparent, discovered by Fuchs [Eq. (4) below]. When all parameters of this linear equation are real, the ratio $f$ of any two linearly independent solutions of (4) maps the upper half-plane onto a circular pentagon of a special kind: it is a circular quadrilateral, (or triangle, or digon) with a slit. We call such circular pentagons *special pentagons*. Simple examples of special pentagons can be seen in Figs. 9, 10a, c, 12a, c, 13a, c, e, g and 14.

All our results are stated in terms of these special pentagons corresponding to particular solutions. The monodromy of Eq. (4) is easily recovered from the pentagon. Construction of the pentagon from the monodromy is described in "Appendix I".

If the $f$-preimage of the tip of the slit is not counted as a vertex, our special pentagon can be considered as a conformal quadrilateral. A real solution of PVI describes the relation between the conformal modulus of this quadrilateral and the $f$-preimage of the tip of the slit. For some values of the modulus the slit vanishes or becomes a cross cut, and the pentagon becomes a circular quadrilateral. These values of the modulus correspond to special points of the PVI solution. Thus the study of the number and mutual position of these special points is equivalent to a geometric problem of describing the evolution of a one-parameter family of special pentagons.

At a special point, the pentagon undergoes one of the four possible transformations, which are described in Sect. 7.

Our algorithm consists of drawing a sequence of special pentagons according to these transformation rules. As the sides of the pentagons belong to fixed circles that do not change under our transformations, the algorithm is of purely combinatorial nature.

More precisely, the algorithm can be described as follows:

We start with a special pentagon. Then we shorten or lengthen the slit. When the slit shortens and vanishes, or when it lengthens, hits the boundary and splits the pentagon, several cases may occur:

(a) the conformal modulus degenerates, which means that $x \to 1$ or $x \to +\infty$, and the algorithm stops.
(b) the conformal modulus does not degenerate, in which case we apply one of the transformations 1–4 described in Sect. 7, and repeat the procedure with the new special pentagon.

To each transformation 1–4 of Sect. 7 corresponds a special point.

In the simplest cases, our pentagons are subsets of the sphere, so drawing them presents no difficulty. In the general case, the pentagons are not subsets of the sphere (their angles and sides can be arbitrarily large), and one needs a special tool for describing them.

We do this using a representation of circular polygons by cell decompositions of a disk which are called nets. This method was developed in [10,11,14–16] for other problems.

We are grateful to C.-S. Lin who shared with us the result from his unpublished preprint [6] which stimulated this paper. We also thank Philip Boalch, Galina Filipuk, Alexander Its, Maxim Kontsevich, Oleg Lisovyy, Yan Soibelman and Vitaly Tarasov for illuminating discussions of PVI, and the anonymous referees whose suggestions improved the exposition.

## 1. A Class of Linear Differential Equations

We consider the class of linear differential equations (1) of the form

$$w'' - \left( \frac{1}{z-q} + \sum_{j=1}^{3} \frac{\kappa_j - 1}{z - t_j} \right) w' + \left( \frac{p}{z-q} - \sum_{j=1}^{3} \frac{h_j}{z-t_j} \right) w = 0, \tag{4}$$

where

$$(t_1, t_2, t_3) = (0, 1, x), \tag{5}$$

$x > 1$, $\kappa_j \geq 0$, $p$ and $q$ are real numbers. We impose the following conditions:

(a) $\infty$ is a regular singularity, with exponent difference $\kappa_4 \geq 0$,
(b) $q$ is an apparent singularity, but the singularities at $(0, 1, x, \infty)$ are not apparent (have non-trivial local projective monodromy).

It follows from the form of (4) that the exponents at $q$ are 0 and 2, and $t_j$ are regular singularities with exponents 0 and $\kappa_j$ for $1 \leq j \leq 3$. The exponents at $\infty$ are determined from the Fuchs relation and from the assumption that their difference is $\kappa_4$.

Conditions (a), (b) determine the $h_j$ uniquely in terms of $p, q, x$ and $\kappa_j$, $1 \leq j \leq 4$, by solving the following system of linear equations:

$$\sum_{j=1}^{3} h_j = p, \tag{6}$$

$$\sum_{j=1}^{3} t_j h_j = pq + \frac{\kappa_4^2 - 1}{4} - \frac{1}{4} \left( \sum_{j=1}^{3} \kappa_j \right)^2 + \frac{1}{2} \sum_{j=1}^{3} \kappa_j, \tag{7}$$

$$\sum_{j=1}^{3} \frac{h_j}{q - t_j} = p^2 - p \sum_{j=1}^{3} \frac{\kappa_j - 1}{q - t_j}. \tag{8}$$

Equations (6) and (7) correspond to condition (a), while Eq. (8) corresponds to condition (b).

The determinant of this system is

$$\frac{x(x-1)}{q(q-1)(q-x)},$$

thus for given real $\kappa_j \geq 0$, $p$, $x \notin \{0, 1\}$, and $q \notin \{0, 1, x\}$ the coefficients $h_j$ are uniquely defined real numbers. Our notation in (2) and (4) is the same as in [28], but we notice a misprint in the first line of [28, (2.1)]: $q$ must be $q_x$.

## 2. Isomonodromic Deformation and PVI

Let us choose the generators $\gamma_j$ of the fundamental group of $\Omega = \mathbf{C} \backslash \{0, 1, x\}$, so that $\gamma_1 \gamma_2 \gamma_3 \gamma_4 = 1$, as shown in Fig. 1.

Let $(w_1, w_2)$ be a pair of linearly independent solutions of (4) normalized by

$$\begin{pmatrix} w_1(x_0) & w_2(x_0) \\ w_1'(x_0) & w_2'(x_0) \end{pmatrix} = I. \tag{9}$$

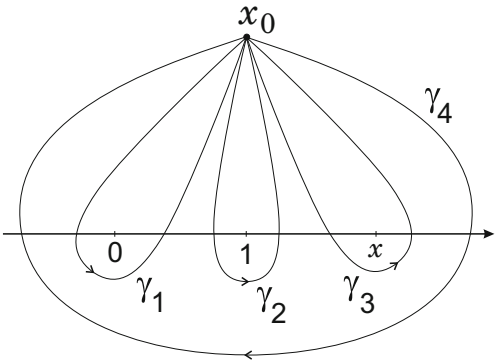


**Fig. 1.** Loops defining $M_1$, $M_2$, $M_3$, and $M_4$

Performing an analytic continuation of these solutions along an element $\gamma \in \pi_1(\Omega, x_0)$ we obtain

$$(w_1^\gamma, w_2^\gamma) = (w_1, w_2)M_\gamma$$

for some $M_\gamma \in GL(2, \mathbf{C})$. Notice that the map $\gamma \mapsto M_\gamma$ is an anti-representation of the fundamental group.[1]

For the ratio $f = w_1/w_2$ we obtain

$$f^\gamma = T_\gamma \circ f,$$

where $T_\gamma$ is a linear-fractional transformation. We identify the group of linear-fractional transformations with $PSL(2, \mathbf{C}) = SL(2, \mathbf{C})/\{\pm I\}$, and the quadruple $(T_1, T_2, T_3, T_4)$ is the set of generators of the *projective monodromy representation* $\pi_1(\Omega, x_0) \to PSL(2, \mathbf{C})$. The correspondence $\gamma \to T_\gamma$ is a group homomorphism. The generators are chosen so that

$$T_1T_2T_3T_4 = \mathrm{id}, \tag{10}$$

and we assume that

$$T_j \neq \mathrm{id}, \quad 1 \leq j \leq 4. \tag{11}$$

For the matrices representing the generators $T_j$ we use the same letters, and they are related to the matrices $M_j$ by

$$T_j = \frac{1}{\sqrt{\det M_j}} M_j^{\mathrm{T}}, \quad 1 \leq j \leq 4,$$

where T stands for the transposition.

When the parameters $\kappa_j$ are fixed, the projective monodromy representation of Eq. (1) depends on $x$, $p$ and $q$.

[1] For the fundamental group we use the standard notation: product $\gamma_1\gamma_2$ means that the path $\gamma_1$ is followed by the path $\gamma_2$.

When we change $x$ and deform the loops continuously, the condition that the monodromy matrices do not change is that $p = p(x)$ and $q = q(x)$ satisfy the following non-autonomous Hamiltonian system [28, (3.7)]:

$$\frac{dq}{dx} = \frac{\partial h}{\partial p}, \quad \frac{dp}{dx} = -\frac{\partial h}{\partial q}.$$

Here the Hamiltonian $h = h_3$ [see (4) for the definition of $h_3$] is given by

$$\begin{aligned} x(x-1)h = {} & q(q-1)(q-x)p^2 \\ & - \{(\kappa_3 - 1)q(q-1) + \kappa_1(q-1)(q-x) + \kappa_2 q(q-x)\}\, p \\ & + \kappa_0(\kappa_0 + \kappa_4)(q-x), \end{aligned}$$

where

$$\kappa_0 = (1 - \kappa_1 - \kappa_2 - \kappa_3 - \kappa_4)/2.$$

This Hamiltonian system is equivalent to (2). All solutions of PVI are obtained in this way.

Special points of $q(x)$ correspond to collisions of the singular point $q$ with one of the four other singular points of Eq. (4). Thus when $x$ is a special point, (4) becomes an equation with four regular singularities (Heun's equation).

In this paper we consider parameters $\kappa_j \geq 0$, $1 \leq j \leq 4$, and real solutions $q(x)$ of (2) defined for $x \in (1, +\infty)$. In view of the formulas (6), (7), (8), in this case all parameters in (4) are real.

The condition on the monodromy matrices that ensures that the solution of PVI is real is discussed in "Appendix I".

*Remark.* A more general class of real Eq. (2) is obtained by allowing some $\kappa_j$ be pure imaginary. In this case, Eq. (4) also has a geometric interpretation [41], but very different from the interpretation in this paper: the developing map $f$ (defined in the next section) still maps the upper half-plane onto a Riemann surface bounded by four circles, but when some $\kappa_j$ are imaginary, this Riemann surface has infinitely many sheets.

## 3. Circular Polygons

*A circular n-gon* is a bordered surface homeomorphic to a closed disk, spread over the sphere without ramification points in the interior, and such that the border consists of $n$ arcs and $n$ points separating them, so that each arc projects into a circle on the sphere locally injectively.

Some circular polygons can be visualized as subsets of the Riemann sphere, see Figs. 12, 13 and 15, which represent circular pentagons and quadrilaterals. But this is not always the case, because we allow arbitrarily large interior angles and arbitrarily long sides.

To give a more formal definition, we denote by $S$ the conformal sphere (the unique compact simply connected Riemann surface). A *circle* in $S$ can be defined by using only the conformal structure: it is the set of fixed points of an anti-conformal involution. Conformal automorphisms of $S$ send circles to circles.

Let $\overline{D}$ be a conformal closed disk,[2] and let $\{t_j\}$ be $n$ distinct boundary points enumerated according to the standard orientation of $\partial D$. In what follows we understand the subscript $j$ in $t_j$ and in other similar notations as a residue modulo $n$.

A *developing map* is a continuous function $f : \overline{D} \to S$ which is holomorphic in $\overline{D}\backslash\{t_1, \dots, t_n\}$ and satisfies

$$f'(z) \neq 0, \quad z \in \overline{D}\backslash\{t_1, \dots, t_n\}, \tag{12}$$

$$f(z) = f(t_j) + (c_j + o(1))(z - t_j)^{\alpha_j} \quad \text{as} \quad z \to t_j, \tag{13}$$

where $\alpha_j > 0$ and $c_j \in \mathbf{C}^*$, or

$$f(z) = f(t_j) + (c_j + o(1)/\log(z - t_j) \quad \text{as} \quad z \to t_j, \tag{14}$$

and such that $f([t_{j-1}, t_j])$ are contained in some circles $C_j \subset S$. Here and in what follows we denote by $[t_{j-1}, t_j]$ and $(t_{j-1}, t_j)$ the closed and open arcs of the boundary $\partial D$ beginning at $t_{j-1}$ and ending at $t_j$. Formulas (13), (14) need an evident modification if $f(t_j) = \infty$, or $f(z) = \infty$ in (12). The circles $C_j$ need not be distinct. A *circular $n$-gon* is identified with the ordered set

$$(\overline{D}, t_1, \dots, t_n, f). \tag{15}$$

Sometimes we will omit the word "circular", calling these objects simply polygons (digons, triangles, quadrilaterals, etc.)

Two circular polygons

$$(\overline{D}_1, t_1', \dots, t_n', f_1) \quad \text{and} \quad (\overline{D}_2, t_1'', \dots, t_n'', f_2) \tag{16}$$

are considered *equal* if there exists a conformal map $\phi : \overline{D}_1 \to \overline{D}_2$ such that $\phi(t_j') = t_j''$ and $f_1 = f_2 \circ \phi$. If the last equality is replaced by $f_1 = L \circ f_2 \circ \phi$, where $L \in \operatorname{Aut} S$ then the two polygons are called *equivalent*.

The points $t_j$ are called *corners* and the arcs $(t_{j-1}, t_j)$ *sides* of a polygon. The angle at $t_j$ is defined as $\alpha_j$ in (13), and we set $\alpha_j = 0$ if (14) holds.

*Notice that we measure the angles in half-turns rather than radians.*

We denote by $C_j$ the circle containing $f([t_{j-1}, t_j])$. Then we obtain $n$ labeled circles with the property that

$$C_j \cap C_{j+1} \neq \emptyset, \quad j \in \mathbf{Z}_n. \tag{17}$$

Indeed, $f(t_j)$ belongs to this intersection. Any such sequence of circles will be called an *$n$-circle chain*, or simply a chain when it is clear what $n$ is.

Notice that 0-gons are just disks, while 1-gons are disks with one marked point where the angle is 1.

Sometimes it will be convenient to use a Riemannian metric on our polygons. To introduce it, start with the standard spherical Riemannian metric of curvature 1 on $S$ and pull it back to $\overline{D}$ via $f$. The resulting metric $\rho$ on $\overline{D}$ is a conformal Riemannian metric of curvature 1 on $\overline{D}\backslash\{t_1, \dots, t_n\}$, has conic singularities with the angles $\alpha_j$ at $t_j$, and each side $(t_j, t_{j+1})$ has constant geodesic curvature. All metric spaces with these properties arise from circular polygons.

In what follows the word "distance" will always mean *intrinsic distance*: the infimum of lengths of curves connecting two points, where the length of a curve is measured using the intrinsic metric. The area of an $n$-gon is also measured in the pull-back spherical

[2] The closure of a Jordan region.

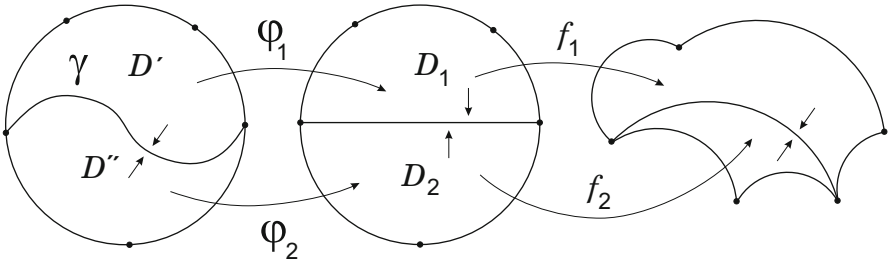


**Fig. 2.** Gluing a quadrilateral and a triangle

metric. It is easy to see that all our polygons have finite areas, moreover, the preimages of points under developing maps are finite.

Polygons are equal if and only if the corresponding metric spaces are isometric. Of course, equivalent polygons may be different as metric spaces.[3]

*3.1. Gluing of two polygons.* We will use the operation of *gluing* circular polygons along a "matching" boundary arc. Suppose that for two polygons in (16), $D_1$ and $D_2$ are the upper and lower halves of the unit disk, the interval $(-1, 1)$ contains no corners of either polygon, and is mapped by $f_1$ and $f_2$ to the same arc of a circle.[4] Then there exist a simple curve $\gamma$ in the unit disk $D$ with endpoints at $\pm 1$ dividing $D$ into two regions $D'$ and $D''$, and conformal homeomorphisms $\phi_1 : D' \to D_1$ and $\phi_2 : D'' \to D_2$ such that $\phi_j(\pm 1) = \pm 1$ and $f_1 \circ \phi_1(z) = f_2 \circ \phi_2(z),\ z \in [0, 1]$, see Fig. 2. Such conformal homeomorphisms $\phi_j$ exist by a theorem of Lavrentiev [21, Ch. VI, §1]. Then

$$f(z) = \begin{cases} f_1 \circ \phi_1(z), & z \in D' \\ f_2 \circ \phi_2(z), & z \in D'' \end{cases}$$

extended by continuity on $\gamma$, is the developing map of a new polygon which is called the gluing of our two polygons along the common boundary arc.

*3.2. Lengthening and shortening of the slit.* Consider an $(n+1)$-gon $Q = (\overline{D}, t_1, \dots, t_n; q, f)$, where the corner $q$ can be anywhere between the $t_j$, this is why we use a different notation for this corner. Suppose that the angle at $q$ equals 2 and the $f$-images of the two sides meeting at $q$ belong to the same circle $C$. (If $q \in (t_{k-1}, t_k)$ then $C = C_k$.) This means that $f$ maps a small neighborhood $V$ of $q$ in $D$ homeomorphically onto a disk centered at $f(q)$ with a slit from the center to the circumference along an arc of the circle $C$.

In this situation we say that the polygon has a slit, and $b := f(q)$ is called the *tip of the slit*. The slit itself is formally defined as follows:

*The slit is the maximal interval* $[t, t']$ *such that* $q \in [t, t'] \subset [t_{k-1}, t_k]$ *and the intrinsic lengths of* $[t, q]$ *and* $[q, t']$ *are equal.*

Examples can be seen in Fig. 3a, c where the tip of the slit is labeled by $q$.

[3] One could use only $PSL(2, \mathbf{C})$-invariant notions, like cross-ratios instead of distances etc., as Klein does. But we find the metric notions more convenient and more intuitive.

[4] This "arc" can be longer than the whole circle. The precise meaning is that there is an increasing diffeomorphism $\psi : [-1, 1] \to [-1, 1]$ such that $f_2(t) = f_1 \circ \psi(t),\ t \in [-1, 1]$.

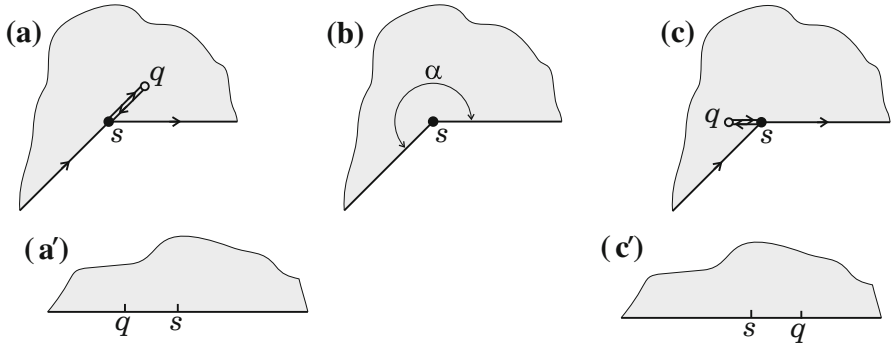


**Fig. 3.** Transformation 1

Consider the small arc $\gamma \subset D$ with endpoints $q$ and $c \in D$ which is defined by $\gamma = f^{-1}(C) \cap V$.

Let $\phi$ be a conformal map of $D$ onto $D\backslash\gamma$. Then $f_1 = f \circ \phi$ defines a new $(n+1)$-gon with corners $t'_j = \phi^{-1}(t_j)$ for $1 \le j \le n$ and $q' := \phi^{-1}(c)$. We say that this new polygon is obtained from the old one by *lengthening the slit*, and the old polygon is obtained from the new one by *shortening the slit*.

Here is an alternative explanation of lengthening or shortening of the slit. Suppose that $D = H$ and $q \in (t_{k-1}, t_k)$. As the sides $(t_{k-1}, q)$ and $(q, t_k)$ are mapped by $f$ to the same circle $C$, we can extend $f$ by reflection to the lower half-plane $H^*$. The resulting function $\tilde{f}$ is meromorphic in $G = H \cup H^* \cup (t_{k-1}, t_k)$, maps $(t_{k-1}, t_k)$ into a circle $C$ and has exactly one simple critical point at $q$. Let $\sigma$ be the reflection in $C$. Choose a small disk $B$ centered at $f(q)$ and let $V \subset G$ be the component of $\tilde{f}^{-1}(B)$ which contains $q$. Let $\psi_s$ be a family of diffeomorphisms of the sphere $S$, which commutes with $\sigma$, whose restriction to $S\backslash B$ is the identity map, and which moves $\tilde{f}(q)$ to a point $s \in C$ near $f(q)$. Then the main existence theorem for quasiconformal mappings in [2] implies that there is a quasiconformal homeomorphism $\phi_s : G \to G$ which commutes with complex conjugation and such that $f_s = \psi_s \circ \tilde{f} \circ \phi_s$ is holomorphic. The restriction of $f_s$ onto $H$ is the developing map of the deformed polygon $Q' = (\overline{H}, t'_1, \ldots, t'_n; q', f_s)$ where $t'_j = \phi_s^{-1}(t_j)$ and $q' = \phi_s^{-1}(q)$. The dependence of $f_s$ on $s$ is real analytic.

Whenever we have a slit it can be lengthened or shortened. This operation does not affect the angles, the chain of the polygon, or the images of the sides other than those two meeting at $q$.

## 4. Relation Between Eq. (4) and a Class of Circular Pentagons

We consider Eq. (4) satisfying conditions (a) and (b) after (4).

**Proposition 1.** *If $p \in \mathbf{R}$, $x > 1$, and $q \in \mathbf{R}\backslash\{0, 1, x\}$, then the ratio $f$ of any two linearly independent solutions of (4) is the developing map of a circular pentagon with $D = H$, and corners at $(t_1, t_2, t_3, t_4) = (0, 1, x, \infty)$ and $q$, with the angles $\kappa_j$ at $t_j$, $1 \le j \le 4$, and 2 at $q$. The $f$-images of the two sides meeting at $q$ belong to the same circle.*

*Conversely, the developing map of every circular pentagon with such properties is the ratio of two solutions of an Eq. (4) satisfying conditions (a), (b), with all parameters real, and $0, 1, x, q$ all distinct.*

*The projective monodromy group of* (4) *consists of the products of even numbers of reflections in the circles containing the $f$-images of the sides of the pentagon. Condition* (11) *holds if and only if no pair of sides meeting at $t_j$, $1 \le j \le 4$, is mapped by the developing map into the same circle.*

Notice that $q$ can be on any of the four intervals $(t_{j-1}, t_j)$, $j \in \mathbf{Z}_4$.

*Proof.* Let $f = w_1/w_2$ be the ratio of linearly independent solutions. Then $f' = (w_1'w_2 - w_1w_2')/w_2^2$, so $f$ is locally univalent in the upper half-plane. If we impose real initial conditions at some real non-singular point, both solutions will be real, and $f$ will be real on the interval between the singularities containing this point. Any other initial condition will give new $f$ related to the old one by a linear-fractional transformation, so $f(z)$ maps every interval between the singular points onto an arc of a circle. The exponents at a singular point $t_j$ are 0 and $\kappa_j$ if $1 \le j \le 4$, so locally $f(z)$ behaves as in (13), (14). At the point $q$, the exponents are 0 and 2, so the angle is 2, and this point is a removable singularity of $f$ by condition (b) after (4), so the sides meeting at $q$ are mapped to the same circle.

For the converse statement, suppose that a circular pentagon with $D = H$ is given, with the angles $(\kappa_1, \kappa_2, \kappa_3, \kappa_4)$ at $(0, 1, x, \infty)$ and 2 at $q$, such that the sides meeting at $q$ are mapped by $f$ into the same circle. Then $f$ extends by reflections to the universal cover of $\mathbf{C}\backslash\{0, x, 1, \infty\}$, and the monodromy of the extended map is a subgroup of $PSL(2, \mathbf{C})$, the group of linear-fractional transformations. This means that the Schwarzian derivative

$$R := \frac{f'''}{f'} - \frac{3}{2}\left(\frac{f''}{f'}\right)^2 \tag{18}$$

is single valued, and the local behavior at $t_j$ and $q$ implies that $R$ has poles of order two with

$$R(z) = \frac{1-\kappa_j^2}{2(z-t_j)^2} + \cdots, \quad \text{as} \quad z \to t_j,$$

$$R(z) = -\frac{3}{2(z-q)^2} + \cdots, \quad \text{as} \quad z \to q,$$

and similarly at infinity, so $R$ is a rational function. As the intervals of the real line between the singularities are mapped to arcs of circles, $R$ is real on the real line. As $t_j$, $q$ and $\kappa_j$ are real, we conclude that the residues of $R$ are also real. Then the general solution of the Schwarz differential equation (18) is a ratio of two linearly independent solutions of (4), see, for example [20,26]. The condition that the images of the sides meeting at $q$ belong to the same circle ensures that $f$ has trivial monodromy at $q$, so $q$ is an apparent singularity with exponents 0 and 2. This completes the proof of Proposition 1.

If $C_k$ is the circle containing $f([t_{k-1}, t_k])$ then $(C_1, C_2, C_3, C_4)$ is a chain of *four* circles for which (17) holds and

$$C_j \ne C_{j+1}, \quad j \in \mathbf{Z}_4 \tag{19}$$

in view of the condition (11). If we denote by $\sigma_j$ the reflection in $C_j$, then the projective monodromy generators are

$$T_j = \sigma_j\sigma_{j+1}, \quad j \in \mathbf{Z}_4. \tag{20}$$

This assumes that the fundamental group generators are chosen as in Fig. 1. To prove (20) we notice that each loop $\gamma_j$, $1 \le j \le 3$, first crosses the interval $(t_{j-1}, t_j)$ from $H$ to the

lower half-plane, and crosses $(t_j, t_{j+1})$ back to $H$. The first crossing corresponds to the reflection $\sigma_j$ and the second to the reflection in the circle $\sigma_j C_{j+1}$. This second reflection is $\sigma_j\sigma_{j+1}\sigma_j$, so the whole continuation around $t_j$ is performed with the reflection

$$\sigma_j\sigma_{j+1}\sigma_j\sigma_j = \sigma_j\sigma_{j+1},$$

as stated. □

If a projective monodromy representation satisfies (20) with some reflections $\sigma_j$, we say that this representation is *generated by reflections*. In "Appendix I" we will find the necessary and sufficient conditions for $T_j$ to be generated by reflections, and will show how to find the $\sigma_j$ when these conditions hold. We will see that the reflections $\sigma_j$ are uniquely defined by the monodromy generators, except in the case when all these generators commute.

## 5. Special Pentagons

The previous section motivates consideration of pentagons with one angle equal to 2, and the sides forming this angle mapped into the same circle by the developing map, while each pair of sides meeting at one of the other corners is mapped by the developing map to distinct circles.

We call them *special pentagons* and use the following notation

$$Q = (\overline{D}, t_1, t_2, t_3, t_4; q, f),$$

where $t_j$ are naturally ordered corners with angles $\alpha_j$, while $q$ is the corner with angle 2 which can lie on any arc between the $t_j$, and the sides meeting at $q$ are mapped by $f$ to the same circle, while the circles containing $f([t_{j-1}, t_j])$ and $f([t_j, t_{j+1}])$ are distinct for all $j \in \mathbf{Z}_4$.

This notation is slightly inconsistent with our general notation for a circular pentagon, because only $t_j$ are listed in their natural order, while $q$ can be on any interval between them. To stress this, we separate $q$ from the $t_j$ by a semi-colon.

We recall that a *conformal quadrilateral*[5] is a simply connected Riemann surface, which is conformally equivalent to a disk, with 4 marked prime ends.[6] Conformal equivalence of conformal quadrilaterals means the existence of a conformal map between them which maps the marked points to the marked points.

Each conformal quadrilateral is conformally equivalent to a rectangle whose marked boundary points are the corners.

We consider special pentagons

$$Q = (\overline{D}, t_1, \ldots, t_4; q, f)$$

as conformal quadrilaterals $(\overline{D}, t_1, \ldots, t_4)$, forgetting the corner $q$, and define the *modulus*

$$\mathrm{mod}\ Q \in (0, \infty)$$

[5] Not to be confused with circular quadrilateral!

[6] For a Jordan region in the plane prime ends are just boundary points. For general simply connected regions we refer to [1].

as the extremal distance in $D$ between the segments $[t_1, t_2]$ and $[t_3, t_4]$ of $\partial D$. For the definition and general properties of the extremal distance we refer to [1] and "Appendix III".

To avoid confusion with the sides of a pentagon as defined before, we use the word *segments* to denote $[t_j, t_{j+1}] \subset \partial D$. Thus one of the segments consists of two sides of the pentagon and contains $q$, while each of the other three segments is the closure of one side of the pentagon.

Every conformal quadrilateral is equivalent to $(\overline{H}, 0, 1, x, \infty)$ for some $x \in (1, \infty)$. With our convention that $(t_1, t_2, t_3, t_4) = (0, 1, x, \infty)$, the modulus is a strictly increasing function of $x$, mapping $(1, +\infty)$ onto $(0, +\infty)$. An explicit expression of this function can be found in [1] but we do not need this formula.

To state the properties of the extremal distance that we need, we use the intrinsic distance on $\overline{D}$ defined in Sect. 3.

**Lemma 1** ([15, Lemma 13.1] and Lemma A4 in "Appendix III"). *Consider a sequence of special pentagons $Q_n$ whose areas are bounded from above. If the intrinsic distance between $[t_1, t_2]$ and $[t_3, t_4]$ tends to zero, while the intrinsic distance between $[t_2, t_3]$ and $[t_4, t_1]$ stays away from zero, then* mod $Q_n \to 0$. *If the intrinsic distance between $[t_2, t_3]$ and $[t_4, t_1]$ tends to 0 while the intrinsic distance between $[t_1, t_2]$ and $[t_3, t_4]$ stays away from zero then* mod $Q_n \to \infty$.

## 6. Local Families of Special Pentagons

We recall that $f(q)$ is called the *tip* of the slit. The slit can be lengthened or shortened with $f(q)$ moving on a circle. Lengthening or shortening the slit along the circle while keeping all circles of the chain unchanged, we obtain a one-parametric family of special pentagons, parametrized by some interval. We choose the length of the slit as parameter.

**Lemma 2.** *As a function of the length of the slit,* mod $Q$ *is monotone. It is strictly increasing if $q \in (t_2, t_3) \cup (t_4, t_1)$ and strictly decreasing if $q \in (t_1, t_2) \cup (t_3, t_4)$.*

This follows from the standard properties of the modulus, [1, 4.3] and Lemma A3 in "Appendix III".

As the slit shortens, it eventually vanishes, and we obtain a polygon with at most 4 sides. As the slit becomes longer, it eventually hits the boundary and becomes a cross-cut which splits $\overline{D}$ into two polygons.

Such a family, obtained from a special pentagon by shortening the slit until it vanishes and lengthening the slit until it hits the boundary, will be called a *local family* of special pentagons. It is parametrized by an open interval (for example, the length of the slit), and corresponds to an open interval on the ray $(1, +\infty)$ in view of Lemma 2.

In the remainder of this section we will study in detail what happens at the ends of a local family. In the next section we will see how local families are combined into a *global family* of special pentagons, parametrized by $x \in (1, +\infty)$, so that the special pentagons of the global family depend continuously and even real-analytically on $x$.

Consider a local family of special pentagons $Q_x$ parametrized by $x \in I$ where $I$ is an interval in $(1, \infty)$.

We say that the modulus *degenerates* if mod $Q_x \to 0$ or mod $Q_x \to \infty$ as $x$ tends to an endpoint of $I$. This means that this endpoint must be 1 or $\infty$.

First we state the conditions of degeneracy.

Suppose that $q \in (t_{k-1}, t_k)$. Suppose that the slit shortens and vanishes, then $q$ must collide with a corner $t_{k-1}$ or $t_k$. If the intrinsic length of $[t_{k-1}, q]$ is strictly smaller than the intrinsic length of $[q, t_k]$ then $q$ will collide with $t_{k-1}$. If the intrinsic length of $[t_{k-1}, q]$ is strictly greater than the intrinsic length of $[q, t_k]$ then $q$ will collide with $t_k$. In both cases we obtain a non-degenerate quadrilateral in the limit, so $x$ tends to some $x_0 \in (1, \infty)$, and $x_0$ is a special point with the value $q(x_0) = t$, where $t \in \{t_{k-1}, t_k\}$ is the corner with which $q$ collided. If the intrinsic lengths of $[t_{k-1}, q]$ and $[q, t_k]$ are equal, then as the slit shortens and vanishes, $t_{k-1}$ and $t_k$ collide, and the limit polygon is a triangle or a digon.

The degeneracy condition is thus the following:

*D1. When the slit shortens and vanishes,* mod $Q_x$ *degenerates if and only if two corners collide in the limit.*

In other words, our special pentagon must be a slit triangle with the slit originating at some vertex $A$, or a slit digon. Notice that the angle of the triangle at $A$ may be an integer, and the images of sides of the triangle which are adjacent at $A$ may belong to the same circle. If this integer is 1 we have a digon instead of a triangle.

Degeneration with shortening slit is illustrated in Fig. 9. When the sit vanishes, two corners at 0 collide.

Now suppose that the slit lengthens. Then eventually it will hit the boundary from inside at some point $s \in \partial H$.

$$\begin{aligned} &\textit{This means that } f(s) \textit{ belongs to the circle of the slit} \\ &\textit{and the intrinsic distance between } q \textit{ and } s \textit{ tends to zero.} \end{aligned} \tag{21}$$

Suppose that $q \in (t_{k-1}, t_k)$. If $s \in [t_{k+1}, t_{k+2}]$, then the modulus degenerates, otherwise it does not. So we have the second degeneration condition:

*D2. When the slit lengthens and splits the pentagon,* mod $Q_x$ *degenerates if and only if the slit hits the segment which is opposite to the segment to which q belongs.*

In other words, in the limit, the slit splits the boundary into two arcs, and the modulus degenerates if and only if the closures of these two arcs contain at least two corners each.

For example, in Fig. 9, when the slit lengthens it eventually splits the pentagon into two triangles. The tip $ik$ of the slit hits the boundary at the point $i$ which splits the side (the half-circle) opposite to the side $(0, ik)$ to which the tip $ik$ belongs.

Now we consider non-degenerate cases, that is the cases when there exists a limit quadrilateral when the slit vanishes or when it splits the pentagon.

**Case 1.** The slit vanishes, $q$ collides with exactly one corner, and the angle of the special pentagon at this corner is positive. See Fig. 3a, b.

**Case 2.** The slit lengthens and hits the boundary at an interior point of the side, splitting the special pentagon into a quadrilateral and a digon with positive angle. See Fig. 4a, b.

It is also possible that as the slit lengthens, it hits the boundary at a corner. If the modulus does not degenerate, this must be a corner neighboring $q$, for example $t_k$. Then the special pentagon splits into a non-degenerate quadrilateral and the remaining part which can have only one corner at $t_k$. Therefore the detached part must be a disk. This we call

**Case 3.** The slit lengthens and hits the boundary at a corner. A disk splits away from the special pentagon, leaving a non-degenerate quadrilateral. See Fig. 5a, b.

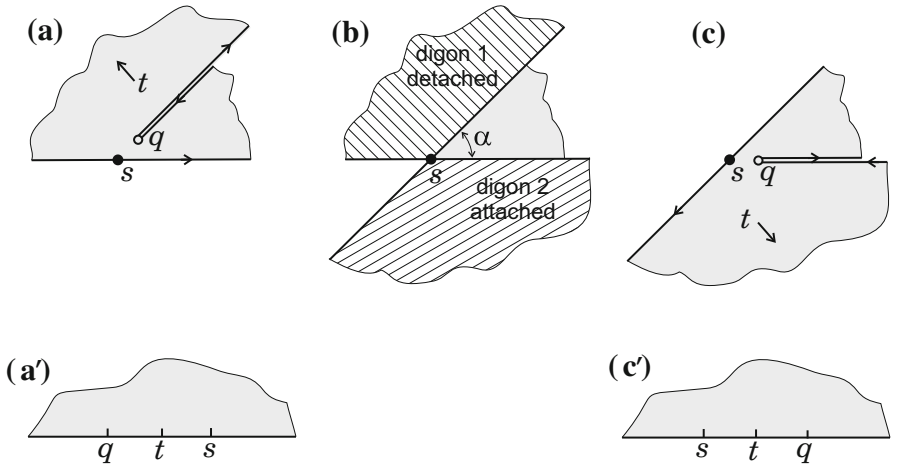


**Fig. 4.** Transformation 2

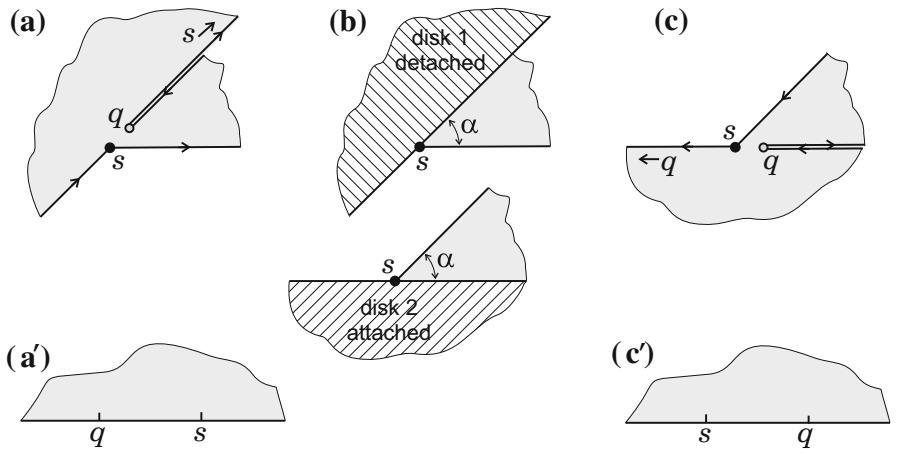


**Fig. 5.** Transformation 3

The remaining cases happen when the slit vanishes as in Case 1, and the corner with which the slit collides has zero angle, or when the slit lengthens, splits the special pentagon, and one part of the split pentagon is a digon with zero angle. These cases will be considered in the next section.

## 7. Transformations Connecting Local Families into a Global Family

In this section we explain what happens when $x$ passes a special point $x_0$, and $q$ passes one of the $t_j$, so that $Q_{x_0}$ is a non-degenerate quadrilateral.

We describe four types of transformations that may occur. The first three correspond to Cases 1, 2 and 3 of the previous section, and the 4-th transformation to the two remaining cases with a zero angle.

*Transformation 1 (Fig. 3). Vanishing slit, Case 1.*

Suppose that $x$ passes a special point $x_0$. Before this $q \in (t_{k-1}, t_k)$, and when $x = x_0$, $q(x_0) = s$, where $s$ is one of the points $t_{k-1},\ t_k$. After $x$ passes $x_0$, $q$ and $s$ interchange. As the images of the sides lie on the same fixed circles, we have the transformation shown in Fig. 3.

*The slit whose image was an arc of a circle vanishes, and then a new slit starts growing with the image on an arc of the circle that is adjacent to the previous circle at the point where the image of old slit vanished.*

The angle $\alpha$ of the limit quadrilateral at the corner where the slit vanishes satisfies

$$\alpha > 1. \tag{22}$$

*Transformation 2 (Fig. 4). The slit hits an interior point $s$ of a segment [see (21)]. The slit is not tangent to this segment (Case 2).*

If the modulus does not degenerate, $s$ must be an interior point of the segment adjacent to that segment which contains $q$. So there is exactly one corner $t$ in the interior of one boundary arc $Z$ between $q$ and $s$, and three corners on the complementary arc. When $q$ hits $s$, our pentagon splits into two polygons: a quadrilateral with the corners $s$ and $t_j \neq t$, and a digon with the corners $s$ and and $t$. Notice that the angles at the two corners of a digon are always equal. It is clear that the angle $\alpha$ of the limit quadrilateral at $s$ is less than 1: it is the inclination of the slit to the side that it hits. Thus

$$\alpha < 1, \tag{23}$$

while the digon has both angles $1 - \alpha$, at $s$ and at $t$.

*When the slit hits the boundary at an interior point of the side, a digon is detached, and a vertical digon*[7] *is attached on the side which was hit. One side of the old slit becomes a side of the new pentagon.*

*Transformation 3 (Fig. 5). The slit hits a corner [see (21)] as described in Case rm 3.*

In this case $s$ is a corner, and there is no other corner on $Z$. When $q$ hits $s$, the special pentagon splits into a quadrilateral with corners at $t_j,\ 1 \leq j \leq 4$ and the other part which must be a disk. So if the limit quadrilateral has angle $\alpha$ at $s$ then the special pentagon before the limit has angle $\alpha + 1$ at $s$.

So far we ignored the non-generic cases which may occur when some circles of the chain are tangent: when the slit vanishes at a corner with zero angle, and when the slit hits from inside a side which is tangent to it. In these cases one more transformation occurs.

*Transformation 4 (Fig. 6). The slit vanishes at a corner with zero angle and a digon with zero angle is attached.*

The slit shortens and vanishes at the corner with zero angle (which is shown at $\infty$ in Fig. 6a, and the resulting quadrilateral in Fig. 6b has angle 1. After that, we attach to this quadrilateral a digon with zero angle (shown as a strip in Fig. 6c, and the slit shortens when $x$ continues to change in the same direction.

When we run $x$ backwards, we first encounter Fig. 6c with the lengthening slit which hits the boundary of the pentagon from inside under zero angle. Similarly to transformation 2, a digon detaches (the strip in Fig. 6c is a digon with zero angle), and a new slit starts growing as in Fig. 6a.

Notice that unlike in all other transformations 1–3, the direction of the slit evolution (whether it lengthens or shortens) does not change for this transformation. Two other distinctions of this transformation from transformations 1–3 are that the old and new

[7] A pair of digons with equal angles formed by two circles are called *vertical*.

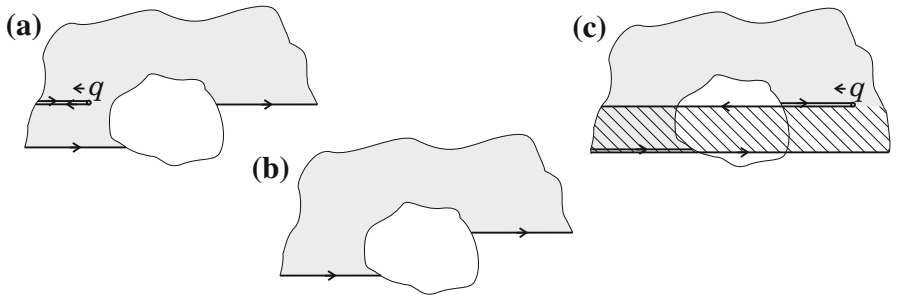


**Fig. 6.** Transformation 4

slit are on the same circle, and that $q$ is on the same segment before and after the transformation.

This is consistent with the fact that the special points of the function $q(x)$ are simple, unless the angle of the special pentagon corresponding to a special point is zero, in which case this special point is a simple critical point for $q(x)$ [22, Ch. 9, §46].

The process we described shows that every local family of special pentagons can be extended to a global family of special pentagons, with the special pentagons becoming quadrilaterals at isolated points. At these points one angle $\alpha$ of the pentagon becomes angle $\beta$ of the quadrilateral, and these angles are related as follows: $\beta = \alpha + 1$ for transformation 1, $\beta = \alpha - 1$ for transformation 3, and $\beta = 1 - \alpha$ for transformation 2.

This continuation can be either performed indefinitely in one or both directions, or the modulus can degenerate at one or both ends.

In Sects. 8, 9 and 10 we will analyse global families.

*Remark.* Transformations 1–4 suggest the following:

*When Eq.* (4) *undergoes an isomonodromic deformation and* $q$ *collides with some* $t_j$*, then the resulting Heun equation has exponent difference* $\pm(\kappa_j + 1)$ *at* $t_j$ *as in Case* 1*, or* $\pm(\kappa_j - 1)$ *as in Cases* 2 *and* 3.

This is true in general, without our restriction that the $\kappa_j$ and $x$ are real. To obtain this result one can use asymptotics of $p(x)$ and $q(x)$ as $x$ tends to a special point written in [38, pp. 534–535], and obtain the limit equation with four singularities directly from (4).

## 8. Explicit Description of Global Families

The previous section shows how local families are combined into a global family. A global family $Q(x)$, $1 < x < +\infty$ consists of local families of special pentagons parametrized by intervals $x_j < x < x_{j+1}$. At the points $x_j \in (1, \infty)$ the special pentagon becomes a non-degenerate quadrilateral. A global family may consist of a single local family; such families will be discussed in Sect. 10. The sequence $x_j$ can be finite, or infinite in one direction, or in both directions. The smallest and the largest terms of this sequence, when they exist, are 1 and $\infty$. All other terms correspond to the special points of the solution of PVI which is described by our global family. To describe global families more precisely, we recall the construction of combinatorial objects related to circular polygons.

## 9. Representation of Polygons by Nets

Circular polygons are conveniently represented by nets [10,15,16]. Consider a polygon given by (15). Its *net* is the cell decomposition of $\overline{D}$ by all $f$-preimages of the circles $C_k$, where $C_k$ is the circle that contains $f([t_{k-1}, t_k])$. The corners are required to be vertices of the net. The 1-cells of the net are labeled by their images. Two nets are considered equal if there is an orientation preserving homeomorphism which maps one onto another preserving the labels of the corners. Let $e_1$ be the 1-cell on the boundary of the net, oriented according to the orientation of the boundary, and beginning at $t_1$. Two polygons with developing maps $f_1$, $f_2$ are equal if their circles $C_j$ are the same, their nets are equal, and the images $e_1$, as oriented 1-cells, are equal.

In the illustrations we label the circles $C_j$ and corresponding 1-cells of the nets with colors (or with different styles of lines in the black and white version).

It is difficult to characterize all possible nets of circular quadrilaterals or special pentagons. The topological classification of generic 4-circle chains is given in "Appendix II". For each type of chain, one has a set of nets compatible with this chain. For the chain topologically equivalent to a quadruple of generic great circles as in Fig. 11, one can give the following characterization of the nets. Notice that the cell decomposition of the sphere in Fig. 11 has the following property which must be inherited by the net:

(a) When two 2-cells share a boundary 1-cell, one of these two cells is a quadrilateral and another is a triangle.

Moreover, the net has an evident additional property:

(b) All interior vertices have degree 4, and all vertices on the sides have degree 3.

Our standing assumption (11) implies that

(c) The degrees of the corners (as vertices of the net) are even.

These three properties completely characterize the nets of circular quadrilaterals over the 4-circle chain shown in Fig. 11. See also Fig. 26a, where the same 4-circle chain is shown. Thus for example, all cell decompositions in the right column of Fig. 23 are nets of quadrilaterals with this 4-circle chain.

## 10. Real Solutions of PVI Without Special Points

Our paper [13] describes all complex solutions of PVI without special points in the complex plane.

In this section we will describe all real solutions of PVI with real parameters, which have no real special points.

For simplicity we limit ourselves to the generic case: all parameters $\kappa_j$ are not integers, and the circles of the chain are not tangent to each other. The last condition holds for example when the projective monodromy contains no parabolic transformations.

Solutions without special points correspond to local families for which the modulus degenerates on both ends. So degeneracy conditions D1 and D2 of Sect. 6 must be satisfied (one condition on one end and another on another end).

Thus we have one of the three configurations shown in Fig. 7.

In a family without special points we must have

$$q(x) \in (t_j, t_{j+1}) \quad \text{for all} \quad x \in (1, \infty)$$

and some $j \in \mathbf{Z}_4$. Suppose without loss of generality that $j = 1$, so that

$$q(x) \in (0, 1), \quad x > 1. \tag{24}$$

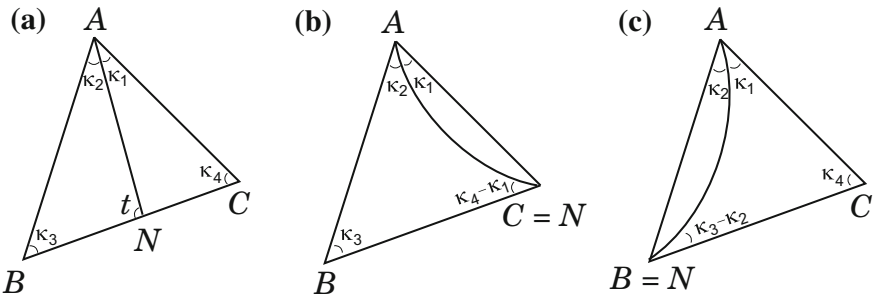


**Fig. 7.** Slit triangles

The condition that $f(0) = f(1)$ when the slit vanishes can be stated in terms of projective monodromy representation:

$$\text{Transformations } T_0 \text{ and } T_1 \text{ have a common fixed point with multipliers } e^{2\pi i\kappa_1} \text{ and } e^{2\pi i\kappa_2}. \tag{25}$$

We will use the results of Klein [31] and Van Vleck [43] on circular triangles. First of all we have

**Lemma 3.** *For any positive numbers $\lambda_j$, $1 \le j \le 3$, there exists a unique equivalence class of circular triangles with angles $(\lambda_1, \lambda_2, \lambda_3)$.*

*Sketch of the proof.* The developing map of a triangle with angles $\lambda_j$ satisfies the Schwarz differential equation:

$$\frac{f'''}{f'} - \frac{3}{2}\left(\frac{f''}{f'}\right)^2 = \frac{1-\lambda_1^2}{2z^2} + \frac{1-\lambda_2^2}{2(z-1)^2} + \frac{\lambda_1^2+\lambda_2^2-\lambda_3^2-1}{2z(z-1)},$$

see, for example, [26, p. 452] or [20, Ch. VI, §3]. Parameters $\lambda_j$ can be arbitrary non-negative numbers, and for fixed parameters all solutions give equivalent triangles. This proves the lemma. □

**Lemma 4.** *In a triangle with angles $(\lambda_1, \lambda_2, \lambda_3)$, the image of the closure of the side opposite to $\lambda_1$ under the developing map makes*

$$E\left(\frac{\lambda_1 - \lambda_2 - \lambda_2 + 1}{2}\right)$$

*full turns*[8] *around the circle containing this image. Here $E(x)$ is the integer part of $x$ for $x > 0$ and zero otherwise.*

This is called the Ergänzungsrelation of Klein [31,43].

First we address the easier cases (b) and (c) in Fig. 7. Consider the case (b). In this case, our triangle $ABC$ is split into two parts, one of which is a digon with both angles $\kappa_1$, and the other part is a triangle with angles $(\kappa_2, \kappa_3, \kappa_4 - \kappa_1)$. The image of a side of a digon cannot cover a full circle. Therefore the image of the side $NA$ of the triangle

[8] When $f : [a, b] \to C$ is an immersion of a closed interval $[a, b]$ into a circle $C$ then the "number of full turns" is defined as card $f^{-1}(a) - 1$.

cannot cover the full circle. The necessary and sufficient condition for this according to Lemma 4 is

$$\kappa_3 + \kappa_1 \le \kappa_2 + \kappa_4 + 1. \tag{26}$$

Similarly, Fig. 7c produces the condition

$$\kappa_4 + \kappa_2 \le \kappa_1 + \kappa_3 + 1. \tag{27}$$

As there are no free parameters in the configurations in Fig. 7b, c, we conclude that when (26) is satisfied, there is a single equivalence class of configurations of the form Fig. 7b and when (27) is satisfied, there is a single equivalence class of configurations of the form Fig. 7c with these angles. This means that each PVI with such parameters has an isolated solution of type (b) or (c), or both. Notice that the two inequalities (26) and (27) cover the whole range of real parameters, so we conclude that isolated solutions of PVI of one or both types Fig. 7b, c always exist. There can be one or two of them.

Now we turn to the case (a). We introduce the auxiliary angle $t \in [0, 1]$ as a parameter (see Fig. 7a).

When $t$ is fixed, there exist two equivalence classes of triangles with prescribed angles: $NAB$ with angles $(t, \kappa_2, \kappa_3)$ and $ANC$ with angles $(\kappa_1, 1 - t, \kappa_4)$. Let $f_1$ and $f_2$ be their developing maps.

The question is when we can glue such two triangles along the side $NA$. As we assume that the circles of the chain are not tangent to each other, $t \in (0, 1)$, and we can post-compose the $f_j$ with linear-fractional transformations to achieve $f_j(N) = 0$, $f_1(BN)$ and $f_2(NC)$ belong to a line $\ell$ through the origin, and $f_j(NA)$ is contained in the real line for $j = 1, 2$. Then it is clear that the necessary and sufficient condition for the possibility of gluing is that the image of the closed side $NA$ under both developing maps intersects the line $\ell$ the same number of times. Indeed, if this is so, the images of the point $A$ under both developing maps are on the same side of the line $\ell$ (or both at 0, or both at $\infty$), and these images can be made equal by additional scaling $z \mapsto rz$ with some $r > 0$.

As $\ell$ intersects the real line at 0 and $\infty$ we are interested in the combined numbers of zeros and poles of $f_j$ on $NA$.

Consider triangle $NAB$ and denote by $(\lambda_1, \lambda_2, \lambda_3)$ the angles at $(N, A, B)$. To count the number of zeros and poles of $f_1$ on $NA$ times the image of $AN$ intersects the circle that contains $NB$ we use the results of Klein [31] (see also [43]) on the number of zeros of hypergeometric function on an interval $[0, 1]$.

We recall that the hypergeometric function $w(z) = F(\alpha, \beta, \gamma, z)$ is the solution of the hypergeometric equation

$$z(z-1)\frac{d^2w}{dz^2} - (\gamma - (\alpha + \beta + 1)z)\frac{dw}{dz} + \alpha\beta w = 0, \tag{28}$$

which satisfies $F(0) = 1$ and is holomorphic at 0. A second linearly independent solution of the same equation is

$$F_1(z) = z^{1-\gamma} F(\alpha - \gamma + 1, \beta - \gamma + 1, 2 - \gamma, z).$$

Thus $F/F_1$ is a developing map of a triangle whose angles are the absolute values of the exponent differences of (28),

$$\lambda_1 = |1 - \gamma|, \quad \lambda_2 = |\gamma - \alpha - \beta|, \quad \lambda_3 = |\alpha - \beta|.$$

We choose

$$\lambda_1 = 1 - \gamma, \quad \lambda_2 = \alpha + \beta - \gamma, \quad \lambda_3 = \alpha - \beta,$$

which defines $\alpha, \beta, \gamma$ uniquely. Notice that $F_1(0) = 0$ because $\gamma \in (0, 1)$. Then $f_1 = F/F_1$ is the developing map of $NAB$, and the side $NA = (0, 1)$.

The number of crossings between $f_1(AN)$ and $\ell$ is equal to the combined number of zeros and poles of $F$ and $F_1$ on $[0, 1]$. We only consider the case $\lambda_1 \in (0, 1)$ which we need.

According to [43] the number of zeros of $F$ on $[0, 1]$ is:

(i) zero, if $[\lambda_2] > [\lambda_3]$,
(ii) $E\left((\lambda_1 + \lambda_3 - \lambda_2 + 1)/2\right)$, if $[\lambda_3] > [\lambda_2]$,
(iii) 0 or 1 depending on whether $E\left((\lambda_1 + \lambda_3 - \lambda_2 + 1)/2\right)$ is even or odd, if $[\lambda_2] = [\lambda_3]$.

The number of zeros of $F_1$ is always

$$E\left(\frac{\lambda_3 - \lambda_1 - \lambda_2 + 1}{2}\right) + 1.$$

Adding these together we obtain that the number of crossings between the image of $AN$ and the circle of $BN$ equals to:

1. if $[\lambda_2] \geq [\lambda_3]$,

and to

$$E\left(\frac{\lambda_1 + \lambda_3 - \lambda_2 + 1}{2}\right) + E\left(\frac{\lambda_3 - \lambda_1 - \lambda_2 + 1}{2}\right) + 1, \quad \text{if} \quad [\lambda_2] < [\lambda_3].$$

Applying this result to $NAB$ and the similar result to $CAN$, (or rather to its mirror image), we obtain that the gluing is possible if and only if one of the following two conditions holds:

(1) $\kappa_2 \geq \kappa_3$ and $\kappa_1 \geq \kappa_4$,
(2) $\kappa_2 < \kappa_3$ or $\kappa_1 < \kappa_4$, and

$$E\left(\frac{\kappa_3 - \kappa_2 + t + 1}{2}\right) = E\left(\frac{\kappa_4 - \kappa_1 - t + 2}{2}\right), \tag{29}$$

and

$$E\left(\frac{\kappa_3 - \kappa_2 - t + 1}{2}\right) = E\left(\frac{\kappa_4 - \kappa_1 + t}{2}\right), \tag{30}$$

To simplify these conditions, we put

$$\begin{aligned} &t = u + 1/2, \quad -1/2 \leq u \leq 1/2, \\ &a = \kappa_3 - \kappa_2 + 1/2, \quad b = \kappa_4 - \kappa_1 + 1/2. \end{aligned} \tag{31}$$

Then conditions (1)–(2) become

(1') $a \leq 1/2$, $b \leq 1/2$, or
(2') $E((a + 1 + u)/2) = E((b + 1 - u)/2)$, and $E((a - u)/2) = E((b + u)/2)$.

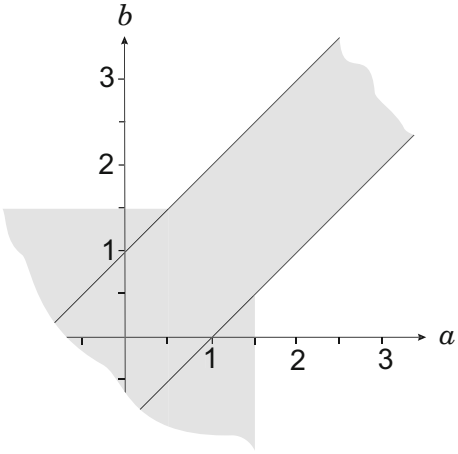


**Fig. 8.** Conditions on $a$ and $b$

Eliminating $u \in (-1/2, 1/2)$ we obtain:

$$|a - b| < 1, \quad \text{or} \quad \min\{a, b\} < 3/2, \tag{32}$$

the shaded region in Fig. 8. For these values of parameters, PVI has an interval of solutions without special points, in addition to one or two isolated solutions of types (b), (c). The boundaries of the regions corresponding to (26) and (27) are shown as lines $a = b + 1$ and $b = a + 1$ in Fig. 8.

**Theorem 1.** *A real solution $q(x)$ of PVI with real parameters $\kappa_j$ defined on $(1, \infty)$ and satisfying $q(x) \in (0, 1)$, $x > 1$ always exists. The monodromy corresponding to this solution satisfies (25). Solutions of type Fig. 7a exist if (32) with a and b as in (31) holds, and these solutions form an interval. Solutions of type Fig. 7b, c exist if (26) or (27) hold, and these solutions are isolated.*

The cases $q(x) \in (t_j, t_{j+1})$ for $j = 2, 3, 4$ are obtained by a cyclic permutation of the angles in our conditions.

In [7], the following theorem is proved: *Solutions of PVI with parameters $(1/2, 1/2, 1/2, 1/2)$ corresponding to unitary monodromy do not have special points on a real interval between the fixed singularities.*

These authors do not assume a priori that their solutions are real. For the case of real solutions, this result can be obtained as follows.

Consider some special pentagon corresponding to a real solution of this equation. The angles are $(1/2, 1/2, 1/2, 1/2, 2)$, and the circles $C_j$ are great circles. Removing the slit we would obtain a geodesic quadrilateral with angles $(1/2, 1/2, 1/2, 3/2)$, or a triangle with angles $(1/2, 1/2, 1)$, but it is easy to see that such quadrilateral does not exist (see for example, [11]). So it must be a geodesic triangle with angles $(1/2, 1/2, 1)$. Then the special pentagon must have the shape as in Fig. 7a, so our global family does not have special points.

In [6], the following fact is proved: *Solutions of PVI with parameters* $(1/2, 1/2, 1/2, 3/2)$ *corresponding to unitary monodromy do not have poles on* $\mathbf{R}\backslash\{0, 1\}$. Again, in the case of real solutions, this follows from our results. When the special pentagon

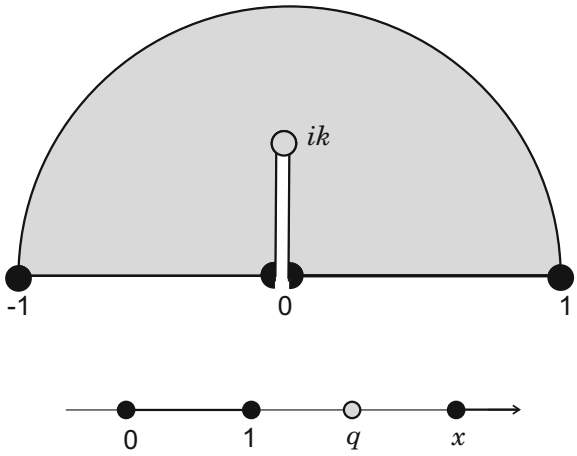


**Fig. 9.** A special pentagon

corresponding to such a solution undergoes a transformation with $q = \infty$ the limit quadrilateral must have angles $(1/2, 1/2, 1/2, 1/2)$ or $(1/2, 1/2, 1/2, 5/2)$. Geodesic quadrilaterals with such angles do not exist [11].

We illustrate Theorem 1 with simple examples. Consider the special pentagon shown in Fig. 9. Here

$$\kappa_1 = \kappa_2 = \kappa_3 = \kappa_4 = 1/2, \tag{33}$$

and the slit is the segment $[0, ik]$. The developing map $f$ maps the upper half-plane conformally onto this pentagon with the boundary correspondence

$$(0, 1, q, x, \infty) \mapsto (-1, 0, ik, 0, 1). \tag{34}$$

The inverse $f^{-1}$ of the developing map sis easy to write explicitly:

$$f^{-1}(z) = \frac{(1 + J(k))(w + J(k))}{(1 - J(k))(w - J(k))}, \quad w = -J\left(\sqrt{\frac{z^2 + k^2}{1 + k^2 z^2}}\right),$$

where

$$J(z) = (z + 1/z)/2$$

is the Joukowski function. This explicit formula gives

$$q = \frac{J(k) + 1}{J(k) - 1}, \quad x = \left(\frac{J(k) + 1}{J(k) - 1}\right)^2.$$

Thus $q(x) = \sqrt{x}$. This is a solution of PVI with parameters (33) which has no special points in the complex plane (all such solutions are listed in [13]). The projective monodromy representation corresponding to this solution is

$$T_0(z) = T_4(z) = 1/z, \quad T_1(z) = T_3(z) = -z.$$

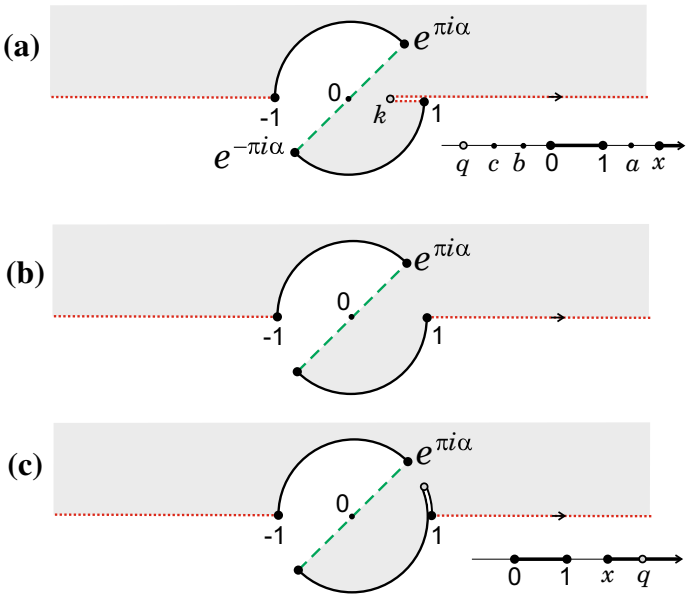


**Fig. 10.** A global family of special pentagons

Changing the boundary correspondence (34) to

$$(0, 1, x, q, \infty) \mapsto (1, -1, 0, ik, 0),$$

we obtain another algebraic solution

$$q(x) = x + \sqrt{x^2 - x}$$

without special points in the whole complex plane [13]. This solution was also obtained in [3, Section 2].

## 11. Another Algebraic Solution

In this section we give another example where everything can be explicitly computed. Consider the region $Q$ in Fig. 10a. Let $f$ be the conformal map of the upper half-plane onto $Q$ with the boundary correspondence

$$(0, 1, x, \infty) \mapsto (-1, e^{i\pi\alpha}, -e^{i\pi\alpha}, 1).$$

These conditions define $x > 1$ uniquely. Let $q = f^{-1}(k)$. Then $q < 0$. As the slit lengthens, the tip $k$ eventually hits 0, the modulus degenerates and we have $x \to +\infty$. As the slit shortens and vanishes, we have transformation 1 occurring for some $x_0 \in (1, +\infty)$. We have $q(x_0) = \infty$. After the transformation we obtain Fig. 10c. When the slit lengthens in Fig. 10c, it eventually hits the boundary at the point $e^{i\alpha}$, the modulus degenerates, and $x \to 1$. Thus in this example we have exactly one special point of $(1, +\infty)$ and this special point is a pole. The monodromy generators of (4) are determined from (20), and we obtain

$$T_1(z) = T_4(z) = 1/z, \quad T_2(z) = e^{-2\pi i\alpha}/z, \quad T_3(z) = e^{2\pi i\alpha}/z.$$

When $\alpha$ is rational, the developing map is an algebraic function, see [12, Section 6]. We set $\alpha = 1/2$. To find $f$ explicitly we denote

$$q = f^{-1}(k), \quad c = f^{-1}(1+i0), \quad a = f^{-1}(0), \quad b = f^{-1}(\infty).$$

Consider the auxiliary function

$$g(z) = -\frac{1}{4}\left(z - \frac{1}{z}\right)^2.$$

It is of degree 4, real on the real and imaginary lines and on the unit circle, and has 6 critical points with critical values

$$g(0) = g(\infty) = \infty, \quad g(\pm 1) = 0, \quad g(\pm i) = 1.$$

Thus the composition $h = g \circ f$ maps the real line into itself and has no critical points in the upper half-plane. This function $h$ extends to the Riemann sphere by symmetry and becomes a rational function. It is easy to see that the real rational function $w = 1 - h$ has:

(i) double poles at $a$ and $b$,
(ii) a simple zero at $x$ and a triple zero at 1,
(iii) $w(1) = w(\infty) = 1$,
(iv) simple critical points at $q$ and $c$, and $w(c) = 0$.

From (i), (ii) and (iii) we conclude that

$$w(z) = \frac{(z-1)^3(z-x)}{(z-a)^2(z-b)^2}, \quad \text{and} \quad x = a^2b^2.$$

Another equation comes from condition (iv) which implies that 0 is a critical value. Solving these two equations with respect to $a$ and $b$ with Maple, we obtain an algebraic solution of PVI with parameters

$$(\kappa_1, \kappa_2, \kappa_3, \kappa_4) = (1/2, 3/2, 1/2, 1/2)$$
$$q(x) = \frac{\sqrt{x} - 3x}{\sqrt{x} - 3},$$

which has a single special point on $(1, +\infty)$, namely a pole at $x = 9$.

## 12. Some Other Cases Where $q(x)$ Can Be Written Explicitly

We mention several special cases without going into detail.

1. Suppose that the projective monodromy representation is reducible. This means that all linear-fractional transformations $T_j$ have a common fixed point. Without loss of generality, we place it at infinity. Then all monodromy transformations are affine, and the circles $C_j$ of the chain are straight lines. Our pentagons are rectilinear and the developing maps can be expressed by the Schwarz–Christoffel formula. Then $q(x)$ can be expressed in terms of hypergeometric integrals.

Indeed, the Schwarz–Christoffel formula of a rectilinear special pentagon gives

$$f(z) = c\int_0^z \zeta^{\alpha_1 - 1}(\zeta - 1)^{\alpha_2 - 1}(\zeta - x)^{\alpha_3 - 1}(\zeta - q)d\zeta = c(I_1(z) - qI_2(z)),$$

where

$$I_1(z) = \int_0^z \zeta^{\alpha_1}(\zeta - 1)^{\alpha_2 - 1}(\zeta - x)^{\alpha_3 - 1} d\zeta$$

and

$$I_2(z) = \int_0^z \zeta^{\alpha_1 - 1}(\zeta - 1)^{\alpha_2 - 1}(\zeta - x)^{\alpha_3 - 1} d\zeta.$$

Normalization $f(1) = a$ and $f(\infty) = b$ will define our special pentagon completely, so we obtain with $k = b/a$

$$q(x) = \frac{kI_1(1) - I_1(\infty)}{kI_2(1) - I_2(\infty)},$$

an expression for $q(x)$ in the form of hypergeometric integrals.

2. Suppose that one of the monodromy transformations is the identity, and the corresponding angle is 1. Then our special pentagon is in fact a slit triangle (or a slit digon, or a slit disk). In this case, the developing map itself can be expressed in terms of hypergeometric functions, see [42], where the case of slit-triangle quadrilaterals has been studied in great detail.

These are the two known cases of reduction of PVI when some solutions can be explicitly found. In a certain sense there are no other cases [45], algebraic solutions and some cases [35] when a solution can be expressed as a somewhat non-standard combination of classical special functions.

## 13. Examples

We begin with the simplest examples when all special pentagons in a global family are regions in the sphere, so the nets are not required for their description.

*Example 1.* The chain of circles corresponding to this example is shown in Fig. 11a. Consider the conformal map $f$ from the upper half-plane onto the shaded region in Fig. 12a. This is the developing map of a special pentagon. The corners on $\partial H$ are shown below, and their images are shown in parentheses.

Suppose that the slit lengthens. Then the extremal distance between the segment $[(0), (1)]$ and the opposite segment $[(x), (\infty)]$ [which contains $(q)$] decreases, so the extremal distance in $H$ between $[0, 1]$ and $[x, \infty]$ decreases, thus $x$ decreases.

When $(q)$ tends to $[(0), (1)]$, modulus degenerates and $x \to 1$.

When the slit shortens, $x$ increases, and eventually the slit vanishes and we obtain Fig. 12b. At this moment $q = \infty$. We have transformation 1, so after that a new slit starts as shown in Fig. 12c and when it hits $[(1), (x)]$, the extremal distance between $[0, 1]$ and $[x, \infty]$ tends to infinity which implies that $x \to +\infty$.

We conclude that solution $q(x)$ of PVI which corresponds to this global family has one pole on $(1, \infty)$, and has no zeros, no fixed points and no 1-points.

For example, this can be any four generic great circles, which corresponds to $SU(2)$ monodromy, determined by formula (20), see "Appendix III".

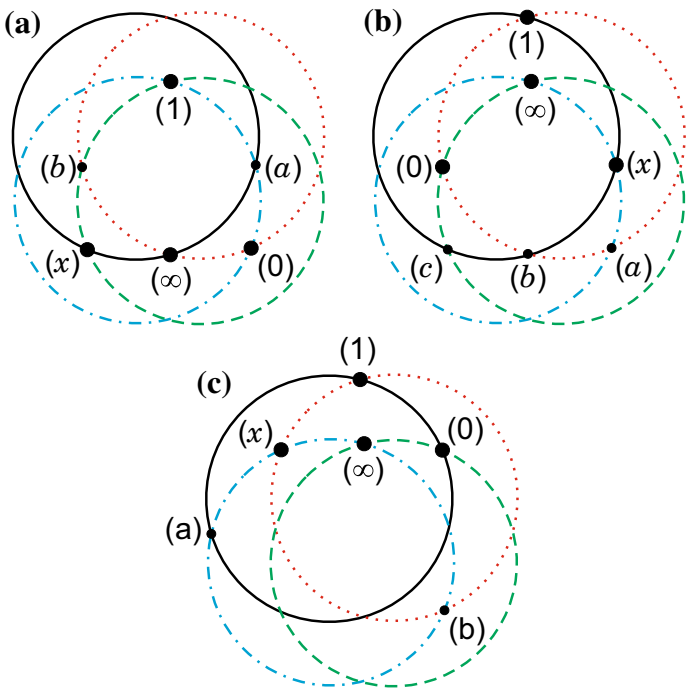


**Fig. 11.** Four-circle chains for **a** Example 1, **b** Example 2, **c** Example 7

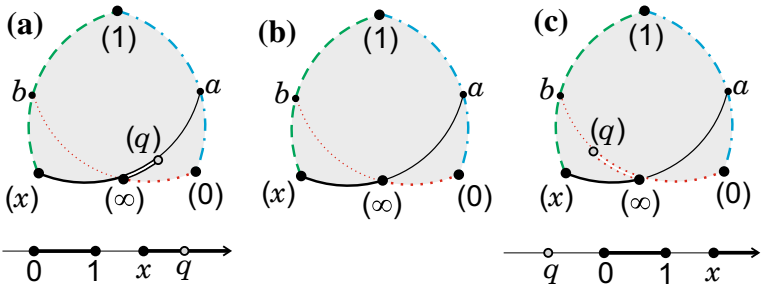


**Fig. 12.** Global family in Example 1

*Example 2.* In this example, Fig. 13, the image of the developing map is also a region in the sphere. In Fig. 13a, when the slit increases, the extremal distance between $[0, 1]$ and $[x, \infty]$ decreases which means that $x$ decreases. When the slit hits the segment $[(0), (1)]$, this distance tends to zero, which means that $x \to 1$.

As the slit in Fig. 13a decreases, $x$ increases, and when the slit vanishes we obtain Fig. 13b. At this moment $q(x) = x$, and we have transformation 1. As $x$ increases further we have Fig. 13c, and then, when $(q)$ hits $[(0), (1)]$, we obtain Fig. 13d. This is transformation 2, and $q(x) = 1$ at this point. The digon on the right of Fig. 13c was detached. According to the transformation 2, we attach to the quadrilateral in Fig. 13d the vertical digon shown on the left of Fig. 13e. The slit in Fig. 13e shortens as $x$ increases. When it vanishes we obtain Fig. 13f where $q(x) = 0$, and we have transformation 2.

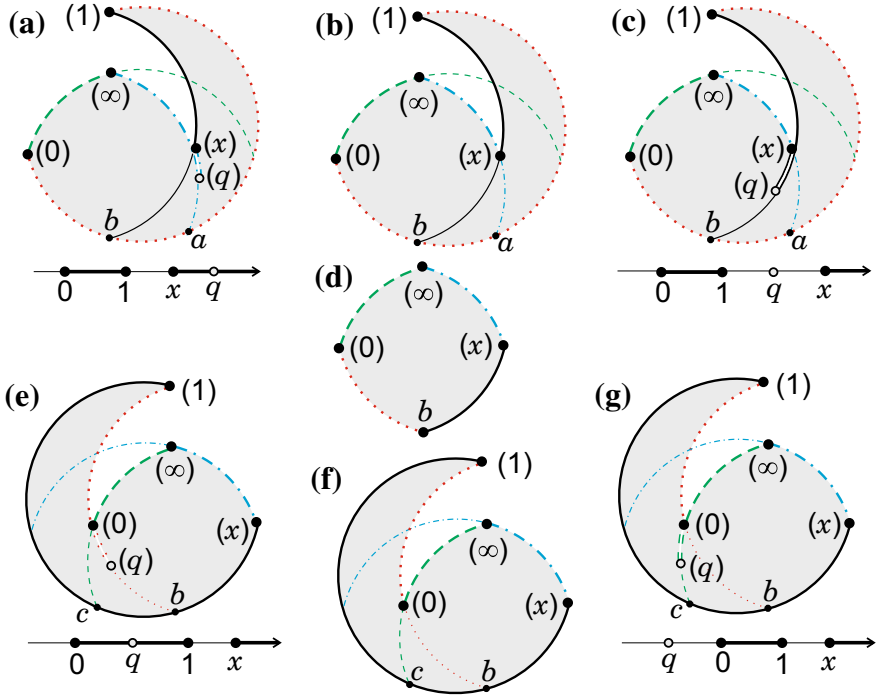


**Fig. 13.** Global family in Example 2

After the transformation we obtain Fig. 13g, where the slit lengthens as $x$ increases. Eventually the slit hits $[(1), (x)]$ which corresponds to $x \to +\infty$.

Therefore, the solution $q(x)$ in this example has three special points $x_1 < x_2 < x_3$ on $(1, +\infty)$, such that $q(x_1) = x_1,\ q(x_2) = 1,\ q(x_3) = 0$. These three special points correspond to quadrilaterals in Fig. 13b, d, f. Monodromy is determined by the four circles in Fig. 11b by formula (20).

*Example 3.* Consider the 4-circle chain shown in Fig. 14, where all pairs $C_j, C_{j+1}$ are tangent. A quadrilateral, which is a subset of the sphere, is the shaded region in Fig. 15b. To obtain a special pentagon we make a slit $[(0), (q)]$ shown in Fig. 15a. When this slit lengthens, it eventually hits the segment $[(x), (\infty)]$ and modulus degenerates, $x \to 1$. As the slit shortens and vanishes in Fig. 15b, we have transformation 4. After that, a digon with zero angle is attached to the shaded region in Fig. 15b along a small arc $[(0), (q)]$ in Fig. 15c, and the new slit $[(q), (1)]$ continues to shorten. The special pentagon in this figure is not a subset of the sphere anymore: the dark shaded area is covered twice. When $(q)$ hits (1), the slit in Fig. 15c vanishes, and a new transformation 4 occurs at a quadrilateral shown in Fig. 15d. Afterwards, a sequence of transformations 4 continues indefinitely, alternately at (0) and (1) with the segments $[1, x]$ and $[\infty, 0]$ of the pentagon increasing by a full circle length after each two transformations, thus $q(x)$ oscillates between 0 and 1 as $x \to +\infty$. The sequence of special points is (0,1, (0,1), …).

*Example 4.* Each special pentagon in this family is mapped by the developing map to a four-circle chain shown in Fig. 16. It is easy to check that Fig. 17b is a net corresponding

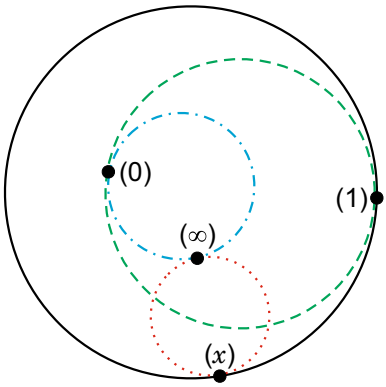


**Fig. 14.** Circles chain for Example 3

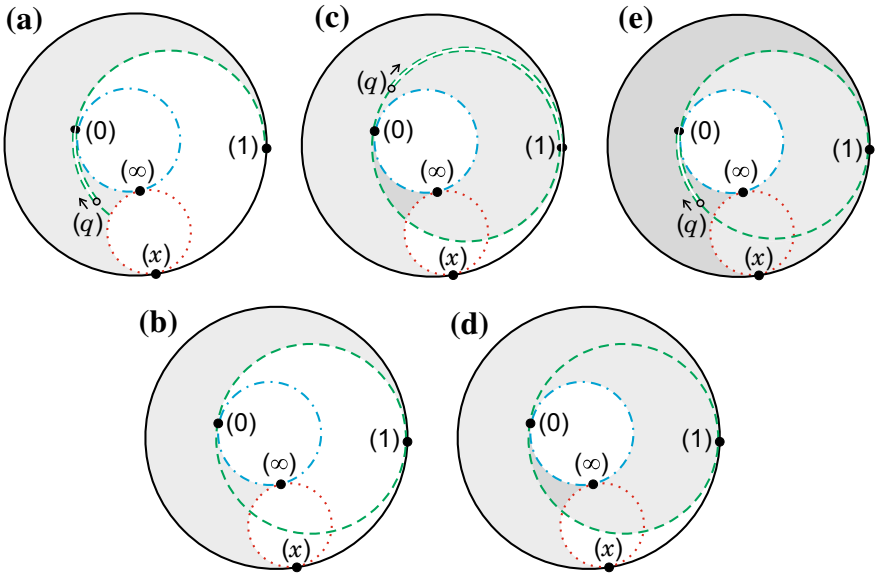


**Fig. 15.** Example 3

to this chain. We make a cut as shown in Fig. 17a, and start a global family from this local family.

The nets for the global family are shown in Figs. 17 and 18, with the left columns (a, c, e, g, i, k) containing the local families of special pentagons, and the right columns (b, d, f, h, j, l) containing quadrilaterals connecting the local families. Modulus degenerates on one end ($x \to +\infty$). As $x \to 1$, we have an infinite chain of local families so as $x$ increases we have the following sequence of special points:

$$(\dots, (\infty, \infty, 0, 0), \infty, x)$$

and no 1-points. The sequence has period of length 4, $(\infty, \infty, 0, 0)$ repeated infinitely many times on the left. The monodromy in this example is

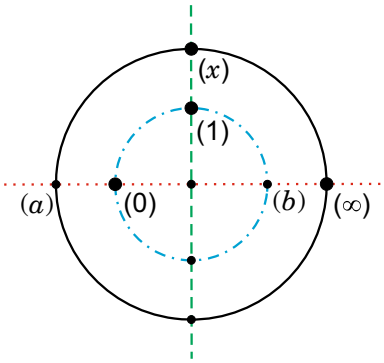


**Fig. 16.** Four-circle chain for Example 4

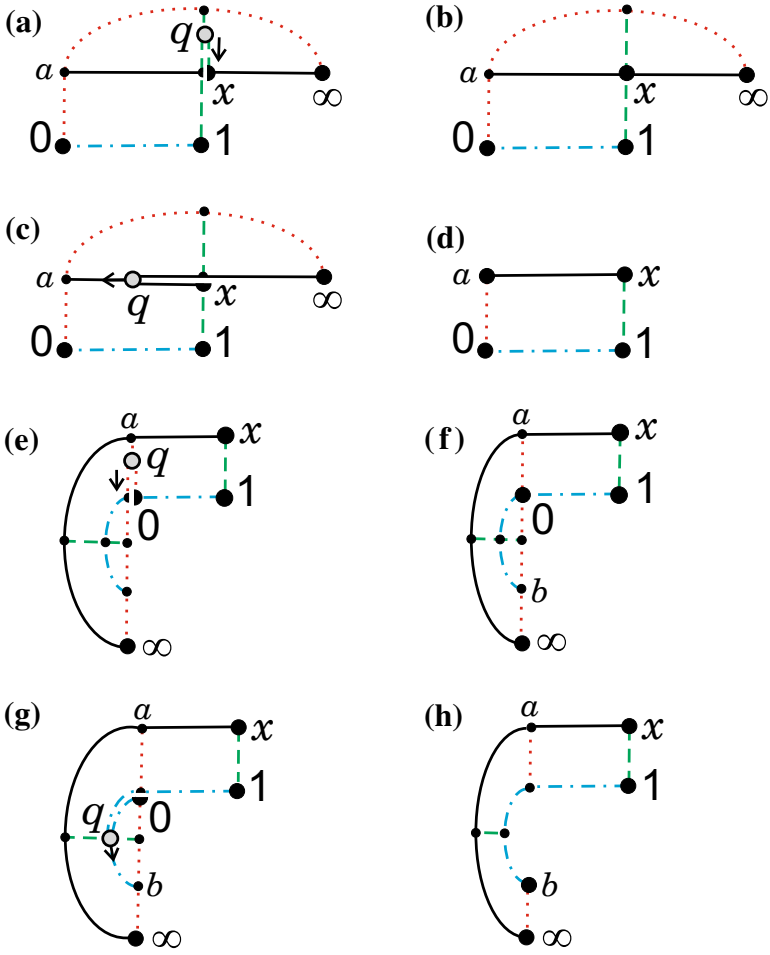


**Fig. 17.** Nets for the global family in Example 4

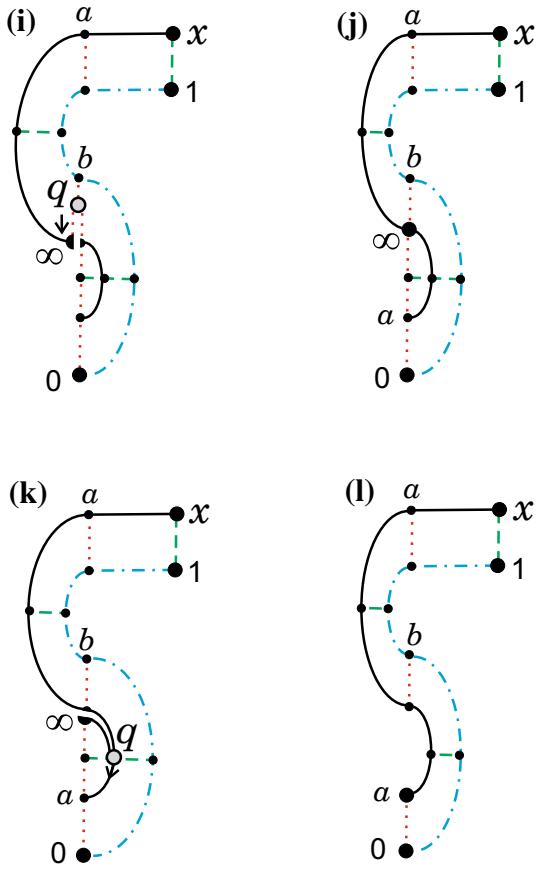


**Fig. 18.** Nets for the global family in Example 4 (continued)

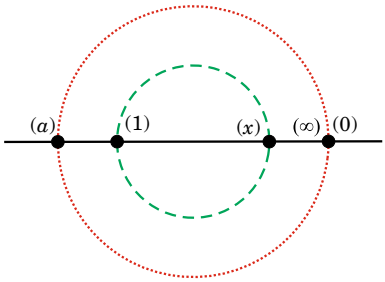


**Fig. 19.** Three-circle chain for Example 5

$$M_0 = \begin{pmatrix} 0 & 1 \\ -1 & 0 \end{pmatrix}, \quad M_1 = \begin{pmatrix} 0 & i \\ i & 0 \end{pmatrix}, \quad M_t = \begin{pmatrix} 0 & Ri \\ Ri & 0 \end{pmatrix},$$

where we assume that the inner and outer circles have radii 1 and $R$.

*Example 5.* Parameters are the same as in the previous example but monodromy is different. The global family is shown in Fig. 20, with the left column (a, c, e, g, i, …)

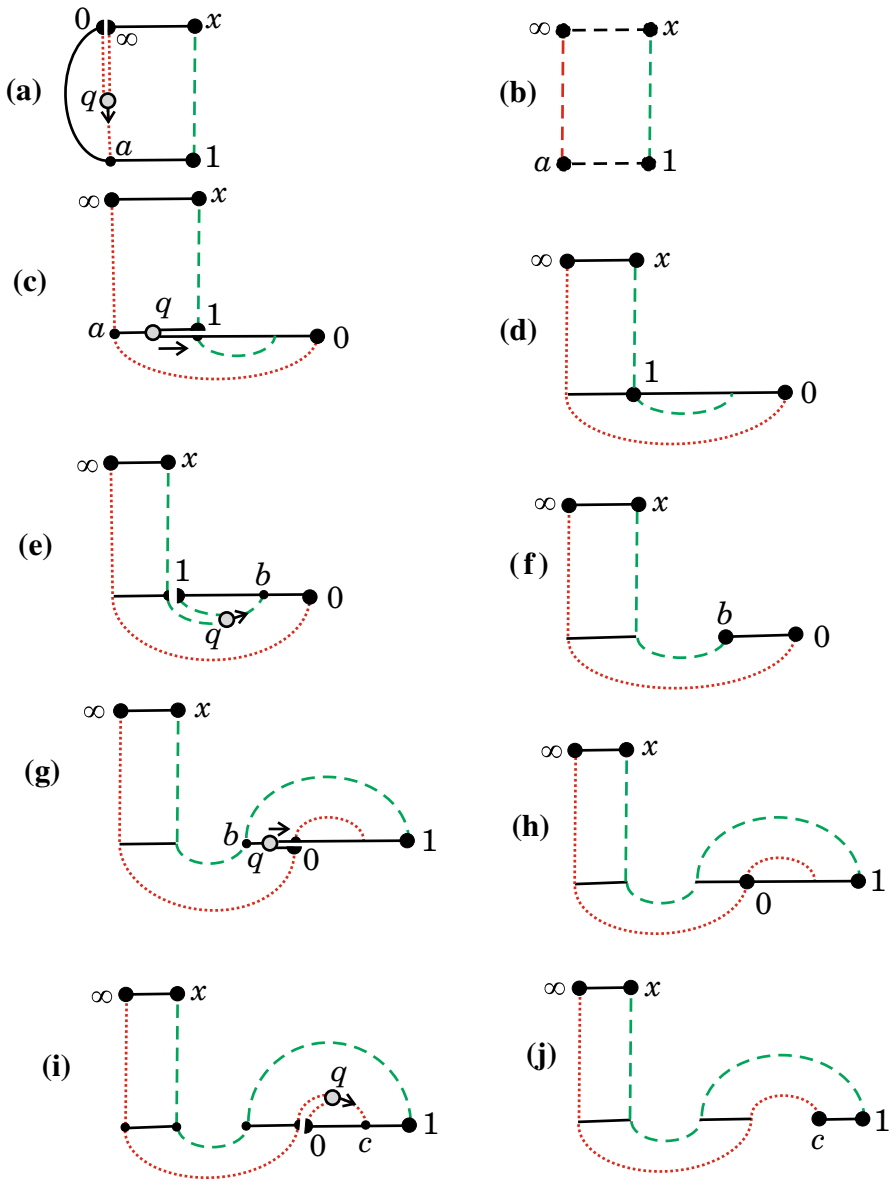


**Fig. 20.** Nets for the global family in Example 5

containing the local families of special pentagons, and the right column (b, d, f, h, j, …) containing quadrilaterals connecting the local families. The corresponding three-circle chain is shown in Fig. 19b. There is an infinite sequence of local families; as $x$ increases from 1 to $\infty$ we have the following sequence of special points:

$$(0, (1, 1, 0, 0), \ldots).$$

The sequence has period (1, 1, 0, 0) repeated infinitely many times on the right.

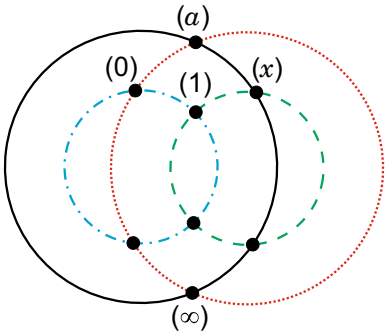


**Fig. 21.** Four-circle chain for Example 6

*Example 6.* The circle chain (see Fig. 21) consists of two pairs of non-intersecting circles. The global family is a doubly infinite sequence. A part of this global family is shown in Fig. 22. It starts with a local family represented by a pentagon in Fig. 22a. As $q$ tends to $a$, this pentagon degenerates to the quadrilateral shown in Fig. 22b. In the opposite direction, when $q$ tends to $x$, the pentagon in Fig. 22a does not degenerate, and the sequence continues indefinitely, with the length of the sides $[1, x]$ and $[\infty, 0]$ ever increasing. At the other end of the sequence shown in Fig. 22, a quadrilateral in Fig. 22j is symmetric with respect to reflection preserving the vertices 1 and $a''$ and exchanging 0 with $x$. The sequence then continues by a local family reflection symmetric to the pentagon shown in Fig. 22i (with the direction of $q$ reversed), and continues indefinitely, with the length of the sides $[0, 1]$ and $[x, \infty]$ ever increasing. We have a doubly infinite sequence of special points

$$(\ldots(\infty, \infty, x, x), \infty, (0, 0, \infty, \infty), \ldots).$$

The sequence is infinite in both directions, has period $(\infty, \infty, x, x)$ on the left and $(0, 0, \infty\infty)$ on the right.

*Example 7.* Consider the 4-circle chain in Fig. 11c. To construct a global family, we begin with a quadrilateral represented by a net in the right column of Fig. 23. That all nets in this column represent some quadrilaterals follows from the criterion given in Sect. 9.

Let us begin with the quadrilateral in Fig. 23b. To transform it to a special pentagon, we make a slit as in Fig. 23a. Lengthening of this slit corresponds to decreasing $x$. In particular, when the slit hits the point $a$ in Fig. 23a, $x \to 1$. Now we follow pictures Fig. 23 alphabetically, in the direction of increasing $x$. So in Fig. 23a the slit shortens. As it vanishes we obtain Fig. 23b, transformation 1 happens, and we pass to Fig. 23c.

In Fig. 23c, the slit lengthens till $q$ hits $b$. A transformation 2 happens, detaching a digon with corners $x$ and $b$ in Fig. 23c to obtain the quadrilateral Fig. 23d. A point $c$ in Fig. 23d maps to the same point as $x$. A digon with the corners $b$ and $c$ is attached to the interval $[b, c]$ of the quadrilateral, resulting in a pentagon Fig. 23e. The slit shortens towards $x$ in Fig. 23e. When it hits $x$, the points $x$ and $c$ collide, and we get a quadrilateral in Fig. 23f. A transformation 1 happens at Fig. 23f, and the slit lengthens towards 1 in Fig. 23g. As it hits 1, a disk with the red (dotted line) boundary is detached, resulting in the quadrilateral Fig. 23h. The point $e$ in Fig. 23h maps to the same point as 1. A transformation 3 happens in Fig. 23h, with a disk with black (solid line) boundary

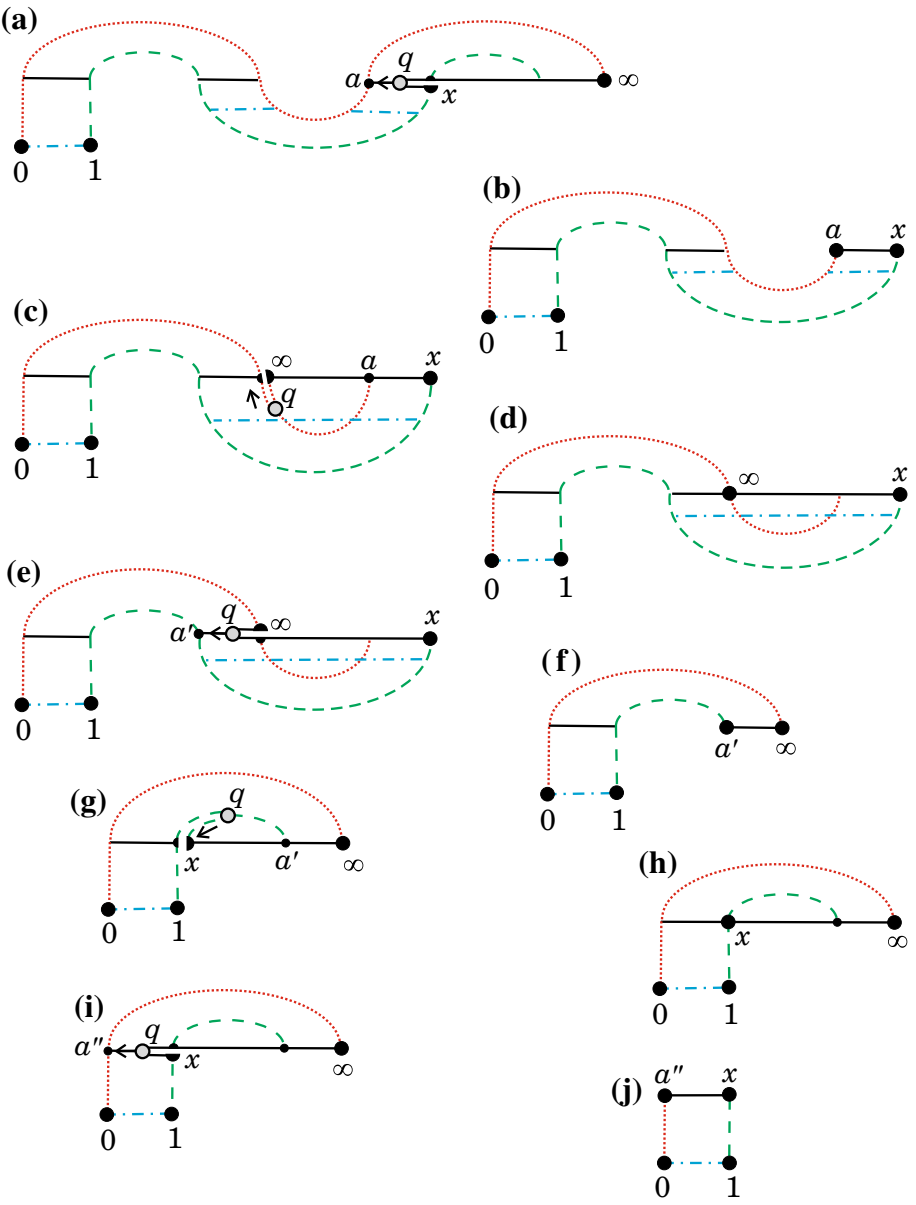


**Fig. 22.** Nets for a part of the global family in Example 6

attached in Fig. 23i. As the slit in Fig. 23i shortens and $q$ hits 1, the points 1 and $e$ collide, and we get the quadrilateral Fig. 23j.

Transformations occurring in the right column of Fig. 23 are: 1, 2, 1, 3, 1. The last quadrilateral shown is Fig. 23j. It is symmetric with respect to the reflection which exchanges 0 and $x$ while leaving 1 and $\infty$ fixed. It is easy to see that in the further continuation of the process we will obtain all pictures Fig. 23 in the reverse order (i)–(a) subject to a reflection exchanging 0 and $x$.

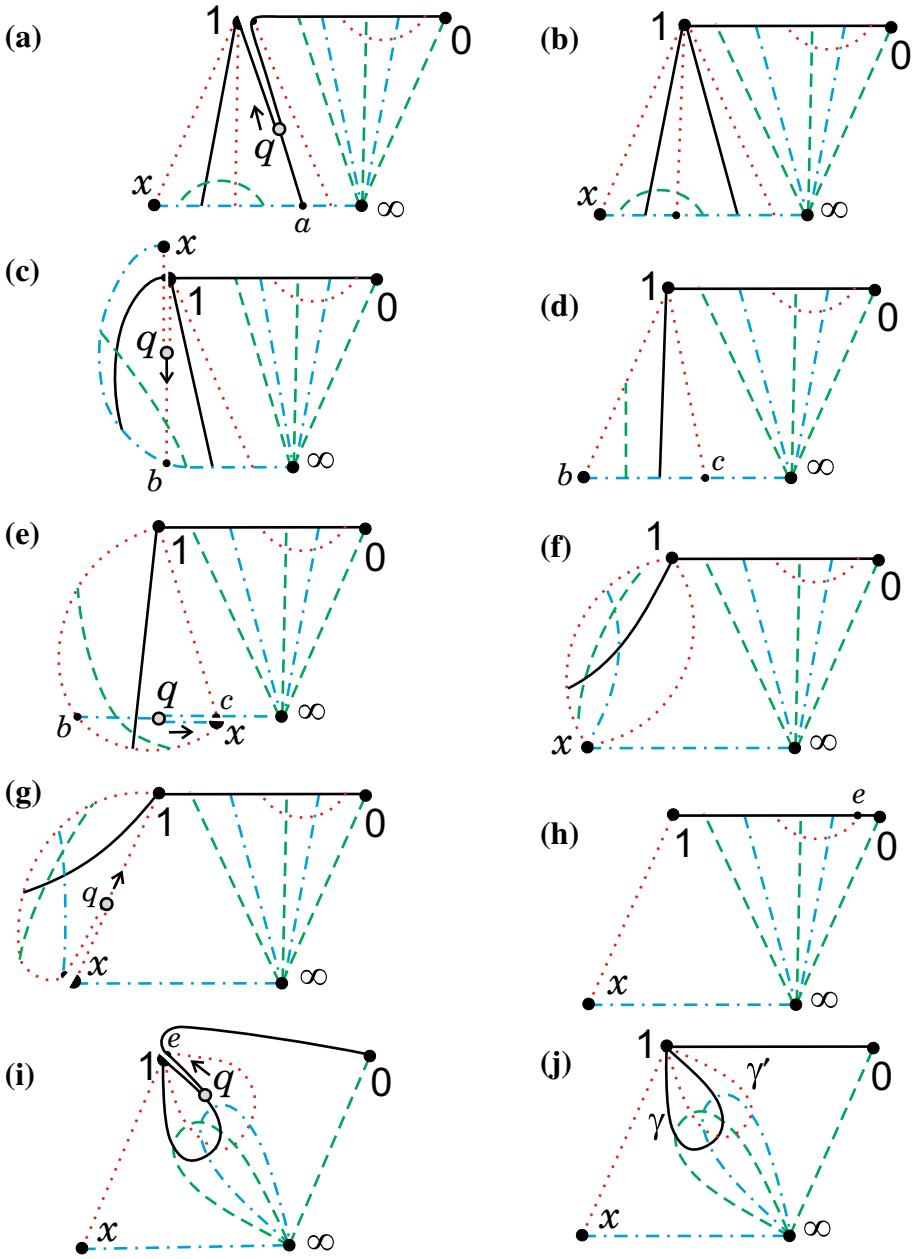


**Fig. 23.** Nets for a half of the global family in Example 7

So Fig. 23 represents only one half of the global family. The global family is symmetric, with the symmetry exchanging (0) and $(x)$. The full sequence of special points is

$$(1, x, x, 1, 1, 1, 0, 0, 1).$$

## Appendix I. Monodromy Representations Corresponding to Quadrilaterals

A monodromy representation consists of 4 matrices in $SL(2, \mathbf{C})$ which satisfy the relation (10). For real equations (4) these four matrices can be represented as products of reflections in the circles $C_j$ containing the images of the sides of a special pentagon. Here we will discuss which monodromy representations correspond to real equations, and how to find the reflections $\sigma_j$ from matrices $T_j$.

This problem was addressed in [8], and we begin by restating the result obtained there. First of all, we change the reference point of the fundamental group in Fig. 1 to the point $-1$ as in Fig. 24, and deform the loops accordingly. Now consider a symmetric set of generators of the fundamental group shown in Fig. 25. Let $N_1, N_2, N_3$ be the monodromy matrices corresponding to $\gamma_1, \gamma_{12}, \gamma_{123}$. We have

$$N_1 = T_1, \quad N_2 = T_1T_2, \quad N_3 = T_1T_2T_3.$$

When none of the $\kappa_j$ is an integer, monodromy representation determines equation (4) uniquely for given real $x$ and $\kappa_j$ [8, 4.2, 4.3]. This implies that monodromy representations correspond to real solutions of (4) normalized as in (9) with $x_0 = -1$ if and only if

$$\overline{N_j} = N_j^{-1}, \quad 1 \le j \le 3, \tag{35}$$

which is equivalent to the condition obtained in [8].

We will derive a different condition, without the assumption on the $\kappa_j$.

Consider an arbitrary quadruple of $SL(2, \mathbf{C})$ matrices satisfying

$$T_1T_2T_3T_4 = \mathrm{id}. \tag{36}$$

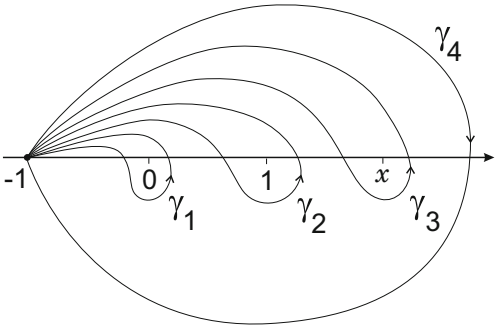


**Fig. 24.** Modified loops

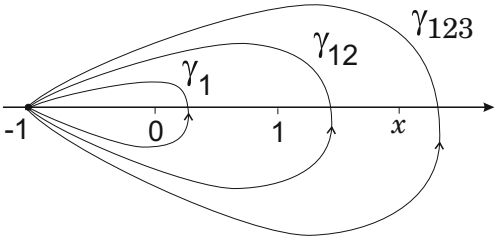


**Fig. 25.** Symmetric loops

$SL(2,\mathbf{C})$ acts on these quadruples by simultaneous conjugation. To parametrize conjugacy classes of monodromy representations we denote

$$t_j = \operatorname{Tr} T_j, \quad t_{jk} = \operatorname{Tr}(T_j T_k) = \operatorname{Tr}(T_k T_j).$$

Conjugacy classes are parametrized by 7 complex numbers

$$t_1,\ t_2,\ t_3,\ t_4,\ t_{12},\ t_{23},\ t_{13} \tag{37}$$

which are subject to one relation

$$\begin{aligned} &t_{12}t_{23}t_{13} + t_{12}^2 + t_{23}^2 + t_{13}^2 \\ &\quad -t_{12}(t_1t_2 + t_3t_4) - t_{23}(t_2t_3 + t_1t_4) - t_{13}(t_1t_3 + t_2t_4) \\ &\quad +t_1^2 + t_2^2 + t_3^2 + t_4^2 + t_1t_2t_3t_4 = 4. \end{aligned} \tag{38}$$

This relation was found by Fricke and Klein [17], and was studied in [4,25] and elsewhere. Parametrization of monodromy representations by these data is discussed in detail in [29]. In particular it is proved there that there are open dense sets on the hypersurface (38) and on the space of conjugacy classes of monodromy representations which are homeomorphic.

We say that a representation is *generated by reflections* if there exist four circles $C_1, C_2, C_3, C_4$ such that the reflections $\sigma_j$ in these circles satisfy

$$T_j = \sigma_j\sigma_{j+1}, \quad j \in \mathbf{Z}_4. \tag{39}$$

Notice that (39) implies (35).

Arbitrary reflection can be written as

$$\sigma(z) = \frac{a\overline{z} + b}{c\overline{z} - \overline{a}}, \tag{40}$$

which we represent by the matrix

$$\begin{pmatrix} a & b \\ c & -\overline{a} \end{pmatrix}, \quad |a|^2 + bc = 1, \tag{41}$$

where $b, c$ are real. Product of reflections represented by matrices $A, B$ is a linear-fractional transformation with matrix $A\overline{B}$. Matrices $A$ associated with reflections are characterized by the properties that $\det A = -1$ and $\overline{A} = A^{-1}$.

Let $\Sigma_j$ be the matrices representing the reflections $\sigma_j$. Then $\Sigma_1 = I$ because of our normalization, and we have $T_1 = \overline{\Sigma_2}$, $T_2 = \Sigma_2\overline{\Sigma_3}$, $T_3 = \Sigma_3\overline{\Sigma_4}$. So $N_1 = T_1$ has matrix $\overline{\Sigma_2}$, $N_2 = T_1T_2$ has matrix $\overline{\Sigma_2}\Sigma_2\overline{\Sigma_3} = \overline{\Sigma_3}$, and $N_3 = T_1T_2T_3$ has matrix $\overline{\Sigma_3}\Sigma_3\overline{\Sigma_4} = \overline{\Sigma_4}$. Thus (35) is satisfied.

Our first question is which representations are generated by reflections.

First we notice that composition of two reflections always has real trace: it is elliptic if the circles cross, parabolic if they are tangent and hyperbolic if they are disjoint. Second, if (39) holds then $T_jT_{j+1} = \sigma_j\sigma_{j+2}$ also has real trace for each $j \in \mathbf{Z}_4$. Thus if (39) holds, the first six parameters in (37) must be real. In addition to this we have the following inequality:

**Theorem A1.** *A monodromy representation* (36) *is generated by reflections if and only if* $t_1,\ t_2,\ t_3,\ t_4,\ t_{12},\ t_{23}$ *are real and*

$$\begin{aligned}\Delta := {} & t_1^2t_3^2 + t_2^2t_4^2 + t_{12}^2t_{23}^2 - 4(t_1^2 + t_2^2 + t_3^2 + t_4^2 + t_{12}^2 + t_{23}^2)\\ & +4(t_1t_2t_{12} + t_2t_3t_{23} + t_1t_4t_{23} + t_3t_4t_{12})\\ & -2(t_1t_2t_3t_4 + t_2t_4t_{12}t_{23} + t_1t_3t_{12}t_{23}) + 16 \le 0. \end{aligned} \tag{42}$$

*Monodromy transformations* $T_j$ *determine the reflections* $\sigma_j$ *uniquely unless all* $T_j$ *commute, and the projective monodromy group is isomorphic to a subgroup of the multiplicative group of the unit circle or of the additive group of the real line.*

*Proof of Theorem A1. Uniqueness.* Suppose that we have (39) and

$$T_j = \sigma_j'\sigma_{j+1}', \quad j \in \mathbf{Z}_4. \tag{43}$$

First we notice that if $\sigma_j = \sigma_j'$ for some $j$, then $\sigma_k = \sigma_k'$ for all $k$. Indeed $\sigma_j = \sigma_j'$ together with (39) and (43) implies $\sigma_{j+1} = \sigma_{j+1}'$ and so on.

Therefore, it is sufficient to prove that $\sigma_2 = \sigma_2'$. We have

$$T_1 = \sigma_1\sigma_2, \quad T_2 = \sigma_2\sigma_3. \tag{44}$$

**Lemma A1.** *If* $T_1$ *and* $T_2$ *are non-identical linear-fractional transformations which together have at least three fixed points, and* (44) *holds, then* $\sigma_2$ *is the reflection in the unique circle which passes through all fixed points of* $T_1$ *and* $T_2$.

*Proof.* If $T_1 \neq \mathrm{id}$ then the circles $C_1$ and $C_2$ of $\sigma_1$ and $\sigma_2$ are distinct and their points of intersection are exactly the fixed points of $T_1$. So $C_2$ contains the fixed points of $T_1$, and $T_2$. This proves the lemma.

How can $T_1$ and $T_2$ have at most 2 fixed points together?

(a) One is elliptic and another one is parabolic, sharing one fixed point.
(b) Both are parabolic.
(c) Both are elliptic sharing two fixed points, in which case they commute.

Consider the case (a). Suppose that the shared fixed point is $\infty$, $T_1(z) = e^{2\pi i\alpha}z$ and $T_2(z) = z + c$. Then $C_1$ and $C_2$ must be lines through the origin, and $C_2, C_3$ must be parallel lines perpendicular to $c$. Therefore $C_2$ is the line through the origin perpendicular to $c$, that is this circle is uniquely defined by $T_1$ and $T_2$.

Now we address (b). If in case (b) $T_1$ and $T_2$ do not share their fixed points, we may assume that $T_1(z) = z + c$ while $T_2$ has fixed point $d \in \mathbf{C}$. Then $C_2$ is the unique line through $d$ perpendicular to $c$.

If the parabolic transformations in (b) share the fixed point, then they are simultaneously conjugate to $z + a$ and $z + b$, and $C_2$ is a line perpendicular to both $a$ and $b$, so $a$ and $b$ are collinear.

So either the circle $C_2$ is uniquely defined by $T_1, T_2$, or $T_1$ and $T_2$ commute, and either both are elliptic or both are parabolic. If they are both parabolic, their families of invariant circles must be the same.

This argument applies to every pair $T_k, T_{k+1}$. Therefore, the only cases when the $\sigma_j$ are not defined by the $T_j$ are the cases stated in the theorem. This completes the proof of uniqueness.

*Existence.* We have already noticed that reality of $t_1, \dots, t_4,\ t_{12},\ t_{23}$ is necessary for (39). It remains to prove that when these traces are real, inequality (42) is necessary and sufficient.

We write a reflection as in (40), (41) In particular, we obtain the reflection in the real axis when $a = i,\ b = c = 0$, and in the line $e^{i\alpha}$ when $a = ie^{i\alpha},\ b = c = 0$.

The trace of a product is

$$\operatorname{tr}(\sigma_1\sigma_2) = 2\operatorname{Re}(a_1\overline{a_2}) + b_1c_2 + c_1b_2. \tag{45}$$

We normalize by $SU(2)$ conjugation so that two adjacent circles are the real line and the line $\{re^{i\alpha} : r \in \mathbf{R}\}$, and write the four matrices of reflections that we want to find as

$$\begin{pmatrix} a_1 & b_1 \\ c_1 & -\overline{a_1} \end{pmatrix}, \quad \begin{pmatrix} ie^{i\alpha} & 0 \\ 0 & ie^{-i\alpha} \end{pmatrix}, \quad \begin{pmatrix} i & 0 \\ 0 & i \end{pmatrix}, \quad \begin{pmatrix} a_2 & b_2 \\ c_2 & -\overline{a_2} \end{pmatrix},$$

in this order. We can further normalize, and assume that 1 is a fixed point of the product of the third and fourth reflections:

$$\frac{i\overline{a_2}z + ib_2}{ic_2z - ia_2} = z, \quad \text{where} \quad z = 1, \tag{46}$$

which gives

$$c_2 - b_2 = 2\operatorname{Re} a_2. \tag{47}$$

Now we write that the traces of products are given (real) numbers:

$$2\operatorname{Re}(-ie^{-i\alpha}a_1) = t_1, \tag{48}$$
$$2\cos\alpha = t_2, \tag{49}$$
$$2\operatorname{Re}(i\overline{a_2}) = t_3, \tag{50}$$
$$2\operatorname{Re}(a_2\overline{a_1}) + b_2c_1 + c_2b_1 = t_4, \tag{51}$$
$$2\operatorname{Re}(-ia_1) = t_{12}, \tag{52}$$
$$2\operatorname{Re}(ie^{i\alpha}\overline{a_2}) = t_{23}. \tag{53}$$

Equations (47)–(53) are easy to solve. First, $a_1$ is determined from (48), (52) and $a_2$ from (50), (53). Then products $b_jc_j$ are found from

$$b_1c_1 = 1 - |a_1|^2, \quad b_2c_2 = 1 - |a_2|^2, \tag{54}$$

which express the fact that determinants of our matrices are $-1$, and together with (47) and (51) permits to find $b_j, c_j$. This amounts to solving two quadratic equations. One of them always has real solutions. Inequality (42) comes from the condition that the second also has real solutions, namely that all $b_j, c_j$ are real.

We give the details of the computation. From (48), (52),

$$-ia_1 = \frac{1}{2}\left(t_{12} - i\frac{t_{12}\cos\alpha - t_1}{\sin\alpha}\right). \tag{55}$$

Similarly, from (50), (53),

$$i\overline{a_2} = \frac{1}{2}\left(t_3 + i\frac{t_3\cos\alpha - t_{23}}{\sin\alpha}\right). \tag{56}$$

Then

$$1 - |a_1|^2 = \frac{1}{t_2^2 - 4}\left(t_1^2 + t_2^2 + t_{12}^2 - t_1 t_2 t_{12} - 4\right), \tag{57}$$

and

$$1 - |a_2|^2 = \frac{1}{t_2^2 - 4}\left(t_2^2 + t_3^2 + t_{23}^2 - t_2 t_3 t_{23} - 4\right). \tag{58}$$

Using (55) and (56) we obtain

$$2\mathrm{Re}\,(a_2\overline{a_1}) = \frac{1}{4 - t_2^2}\left(2t_1 t_{23} + 2t_3 t_{12} - t_1 t_2 t_3 - t_2 t_{12} t_{23}\right), \tag{59}$$

and using (47)

$$c_2 - b_2 = \frac{t_3 \cos\alpha - t_{23}}{\sin\alpha}. \tag{60}$$

Next, from (54), (57), (58), we obtain

$$b_1 c_1 = \frac{1}{t_2^2 - 4}\left(t_1^2 + t_2^2 + t_{12}^2 - t_1 t_2 t_{12} - 4\right), \tag{61}$$

and

$$b_2 c_2 = \frac{1}{t_2^2 - 4}\left(t_2^2 + t_3^2 + t_{23}^2 - t_2 t_3 t_{23} - 4\right). \tag{62}$$

Solving first the system (60), (62) with respect to $b_2, c_2$, we obtain a quadratic equation with discriminant

$$t_2^2 t_3^2 - 4t_2^2 - 4t_3^2 + 16 = (t_2^2 - 4)(t_3^2 - 4) \geq 0,$$

because $t_j \in [-2, 2]$. So we always have real solution $c_2, b_2$.

Next we solve the system (51) with (59) and (61) with respect to $b_1, c_1$, using the known product $b_2 c_2$ from (62). This also leads to a quadratic equation, whose discriminant is a polynomial in $t_{12}$, $t_{23}$ and $t_j$. This polynomial factors (using Maple) with one factor $t_2^2 - 4 < 0$ and the other factor is $\Delta$ in (42).

This completes the proof.

*Remark on the proof.* In the process of recovery of $\sigma_j$ we had to solve two quadratic equations, so in general we had 4 choices to make. On the other hand, our normalization condition (46) leaves two choices because two circles intersect at two points. Next, we never used $t_{13}$ in our recovery procedure for $\sigma_j$. As $t_{13}$ satisfies the quadratic equation (38), assigning $t_{13}$ narrows our choices to two.

An interesting question is what happens when the monodromy group is conjugate to a subgroup of $SU(2)$. Every element of $SU(2)$ is the product of two reflections in great circles. If an element of $SU(2)$ is represented as a product of two reflections, then these reflections must be in great circles, because these circles contain the fixed points of the element which are diametrally opposite.

An interesting special case is when all seven parameters in (37) are real. According to [36, Prop. III.1.1] this happens if and only if he projective monodromy group is a subgroup of $SU(2)$ or $SL(2, \mathbf{R})$. When the group is generated by reflections, the first six parameters in (37) are real, so all seven will be real if and only if the discriminant of (38), as a quadratic equation with respect to $t_{13}$, is non-negative. Straightforward computation shows that this discriminant is nothing but $\Delta$ defined in (42). Thus we obtain

**Theorem A2.** *Let $T_1, T_2, T_3, T_4$ be unitary matrices satisfying (36), and all seven parameters in (37) are real. This representation is generated by reflections if and only if $\Delta = 0$, which is equivalent to*

$$2t_{13} + t_{12}t_{23} - t_1t_3 - t_2t_4 = 0. \tag{63}$$

Equation (63) is what (38) becomes when $\Delta = 0$.

*Remark.* We mention a simple geometric interpretation of our conditions.

Condition that $t_{12}$, $t_{23}$ are real: the trace of a product of two elliptic transformations is real if and only if their four fixed points lie on a circle.

Condition $\Delta = 0$ gives a relation between six angles associated to a spherical or hyperbolic quadrilateral: four angles of the quadrilateral, and two angles between the circles containing the images of opposite sides. These six angles serve as natural parameters: spherical or hyperbolic quadrilaterals with prescribed angles at the corners form a one-parametric family, while circular quadrilaterals with prescribed corners form a two-parametric family.

Theorem A2 can be compared with Jimbo's asymptotics [30]. (A misprint in the main result in [30] was corrected in [5]). It follows from the explicit formula expressing the asymptotics in terms of the monodromy that for $SU(2)$ or $SL(2, \mathbf{R})$ monodromies this asymptotics is real if and only if $\Delta = 0$. For general monodromies (not in $SU(2)$) it is difficult to determine directly when Jimbo's formula gives a real asymptotics.

## Appendix II. Topological Classification of 4-Circle Chains

We recall that a 4-circle chain consists of 4 labeled circles $C_j$ on the Riemann sphere such that

$$C_j \neq C_{j+1}, \quad C_j \cap C_{j+1} \neq \emptyset, \quad j \in \mathbf{Z}_4. \tag{64}$$

In this section we give a topological classification of generic chains. Generic means that there are no tangent circles and no triple intersections. Two chains are considered equivalent if there is an orientation-preserving homeomorphism of the sphere which maps the union of circles of one chain onto the union of circles of another chain.

In fact, we classify generic *unordered* quadruples of circles with the following property: each circle intersects at least two other circles. There are two kinds of such quadruples: those in which each circle intersects all three other circles (see Fig. 26) and those with a pair of non-intersecting circles (see Fig. 27). Note that the quadruples in Fig. 26d and 27k are not reflection symmetric, thus each of them represents two equivalence classes. We omit the elementary but tedious proof that these exhaust all possibilities. To see that all these cell decompositions are distinct we indicated the faces with more than 3 edges in each cell decomposition.

It follows from the classification that the circles in Fig. 26 can be arbitrarily ordered to form a 4-circle chain, while the circles in Fig. 27 form a 4-circle chain when ordered so that non-intersecting circles are not adjacent.

Notice two equivalent reformulations of this problem: topological classification of arrangements of four planes in the hyperbolic space, subject to the intersection condition (64), and topological classification of possible intersections of a sphere with four planes in the Euclidean space, under the condition that the planes $P_j$ can be so ordered that each line $P_j \cap P_{j+1}$ intersects the sphere.

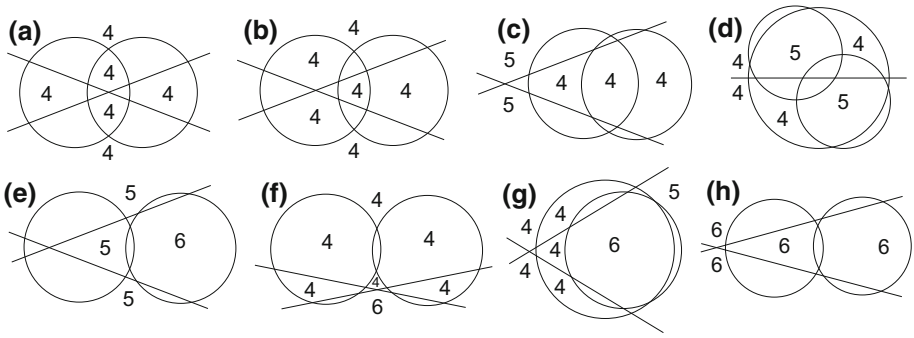


**Fig. 26.** Generic chains **a**–**h**. All pairs of circles intersect

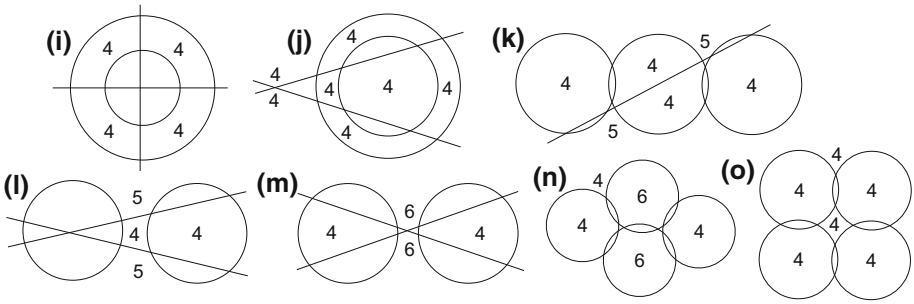


**Fig. 27.** Generic chains **i**–**o**. Some pairs are disjoint

*Remarks and conjectures.* If all pairs of circles in the chain intersect, then there are only finitely many nets on this chain with prescribed angles. This follows from the results of [27]. In this paper, Ihlenburg proves that all circular quadrilaterals can be obtained from finitely many topological types by applying four explicitly defined operations. All these operations do not decrease angles, and three of them increase some angles. The only operation which leaves all angles unchanged requires two disjoint circles in the chain.

It follows that real solutions of PVI corresponding to all chains in Fig. 26 can have only finitely many special points on an interval between fixed singularities. On the other hand, our examples 4, 6 suggest that for all chains containing pairs of disjoint circles the number of special points is infinite. Moreover, it looks like it is infinite in one direction when there is one pair of disjoint circles, and infinite in both directions if there are two such pairs, like in Fig. 21 which is the same as Fig. 27o.

## Appendix III. Moduli of Conformal Quadrilaterals

Consider a closed rectangle $Q$ in the plane with vertices $0, 1, 1 + ia, ia$.

The number $a > 0$ is called the modulus, $a = \mathrm{mod}\, Q$. Any Borel measurable function $\rho(z) \geq 0$ defines a *conformal metric* $\rho(z)|dz|$ on $Q$: the length of a curve $\gamma$ and the area of a set $E \subset Q$ are defined as

$$\ell_\rho(\gamma) = \int_\gamma \rho(z)|dz|, \quad \text{and} \quad A_\rho(E) = \int_E \rho^2(z)dxdy.$$

Let $\Gamma$ be the set of all curves in $Q$ connecting the horizontal sides. Define

$$\ell_\rho(\Gamma) = \inf_{\gamma\in\Gamma} \ell_\rho(\gamma),$$

and

$$\lambda(\Gamma) = \sup_\rho \frac{\ell_\rho^2(\Gamma)}{A_\rho(Q)}, \tag{65}$$

where the sup is taken over all metrics for which the numerator and denominator are finite and not zero.

**Lemma A2.** [2, I.D, Example 1] $\lambda(\Gamma) = a$. *Formula* (65) *defines the* extremal length *of an* arbitrary *family of curves* $\Gamma$ *in* $Q$. *So defined extremal length is a conformal invariant of a family of curves.*

*Let* $\Gamma'$ *be the family of all curves in* $Q$ *connecting the vertical sides. Then evidently*

$$\lambda(\Gamma)\lambda(\Gamma') = 1. \tag{66}$$

*The following comparison inequalities immediately follow the from definition.*

**Lemma A3** [2, I.D, Theorem 2]. *Consider two families of curves* $\Gamma_1$ *and* $\Gamma_2$ *and suppose that every curve* $\gamma_2 \in \Gamma_2$ *contains some curve* $\gamma_1 \in \Gamma_1$. *Then* $\lambda(\Gamma_1) \le \lambda(\Gamma_2)$.

*The assumption means that* $\Gamma_1$ *has "more curves" and the curves of* $\Gamma_2$ *are "longer".*

*For a metric* $\rho$, *the intrinsic distance* $d_\rho(E_1, E_2)$ *between two subsets* $E_1$ *and* $E_2$ *of* $Q$ *is defined as infimum of* $\ell_\rho(\gamma)$ *over all curves connecting a point in* $E_1$ *with a point in* $E_2$.

**Lemma A4.** *Suppose that a metric* $\rho$ *has the following properties:*

$$A_\rho(B(r)) \le Kr^2, \tag{67}$$

*for all* $r > 0$ *and for all intrinsic disks* $B(r)$ *of radii* $r$, *the intrinsic* $\rho$*-distance between the vertical sides is at least* $2c$, *and the intrinsic* $\rho$*-distance between the horizontal sides is less than* $\epsilon/2$.

*Then* mod $Q \le \delta$, *where*

$$\delta = \frac{4(K+1)}{\log(c/\epsilon)} \to 0$$

*as* $\epsilon \to 0$, *for any fixed* $K > 0, c > 0$.

*Proof.* Choose a curve $\gamma_0$ connecting the horizontal sides, and such that $\ell_\rho(\gamma_0) < \epsilon$. Let $P$ be a point on $\gamma_0$. Consider the closed $\rho$-disks $B(\epsilon)$ and $B(c)$ of radii $\epsilon$ and $c$, both centered at $P$. Then $B(\epsilon)$ contains $\gamma_0$. Let $\Gamma'$ be the family of all curves in $Q$ connecting the vertical sides. Every curve $\gamma'$ of this family crosses $\gamma_0$, therefore $\gamma'$ intersects both $B(\epsilon)$ and $Q\backslash B(c)$. Therefore

$$\lambda(\Gamma') \ge \lambda(\Gamma_1), \tag{68}$$

where $\Gamma_1$ is the family of all curves in $Q$ connecting $B(\epsilon)$ with $Q\backslash B(c)$. To estimate $\lambda(\Gamma_1)$ from below, consider the metric $\tau(z)|dz|$ defined by the function

$$\tau(z) = \frac{\rho(z)}{\log(c/\epsilon)d_\rho(z, P)}, \quad z \in B(c)\backslash B(\epsilon),$$

and zero otherwise. For every $\gamma_1 \in \Gamma_1$ we have

$$\ell_\tau(\gamma_1) \geq \frac{1}{\log(c/\epsilon)} \int_\epsilon^c \frac{\rho(z)|dz|}{d_\rho(z, P)} \geq \frac{1}{\log(c/\epsilon)} \int_\epsilon^c \frac{ds}{s} \geq 1.$$

Here we made the change of the variable $s = d_\rho(z, P)$ and used the evident inequality $ds \leq \rho(z)|dz|$.

To estimate the $\tau$-area of $Q$ we define $r_0 = \epsilon,\ r_k = 2^k r_0$, $k = 1, \ldots, N$, $N = [\log_2(c/\epsilon)] + 1$, and let $B_k$ be the $\rho$-disk of radius $r_k$ centered at $P$. Then, using (67), we obtain

$$\begin{aligned} A_\rho(Q) &\leq \frac{1}{\log^2(c/\epsilon)} \sum_{k=1}^N \int_{B_k \setminus B_{k-1}} \frac{\rho^2(z)dxdy}{r_{k-1}^2} \leq \frac{4}{\log^2(c/\epsilon)} \sum_{k=1}^N \frac{A_\rho(B_k)}{r_k^2} \\ &\leq \frac{4KN}{\log^2(c/\epsilon)} \leq \frac{4(K+1)}{\log(c/\epsilon)}. \end{aligned}$$

Thus $\lambda(\Gamma_1) \geq (\log(c/\epsilon))/(4(K+1))$, and using (66) and (68), we obtain

$$\operatorname{mod} Q = \lambda(\Gamma) \leq 4(K+1)/(\log(c/\epsilon)).$$

This proves the lemma. □

The upper half-plane can be mapped conformally onto $Q$ so that

$$(0, 1, x, \infty) \mapsto (0, 1, 1 + ia, ia)$$

by the Schwarz–Christoffel formula. Let

$$\phi(z) = \int_0^z \frac{d\zeta}{\sqrt{z(z-1)(z-x)}}.$$

Then the desired conformal map is $\phi(z)/\phi(1)$, and the modulus $a(x) = -i\phi(\infty)/\phi(1)$. It follows from Lemma A3 that $x \mapsto a(x)$ is increasing homeomorphism of $(1, \infty)$ onto $(0, +\infty)$.

In our applications, the metric $\rho$ arises as a pull-back of the standard spherical metric of curvature 1 on the sphere $S$ by a conformal local homeomorphism $f : Q \to S$. If $f$ is $p$-valent (which means that every point has at most $p$ preimages), then (67) is satisfied with $K = \pi p$. Indeed, for spherical discs on $S$, (67) is satisfied with $K = \pi$ by direct computation, and $f(B(r))$ is evidently contained in a disk of radius $r$ in $S$.

## References


1. Ahlfors, L.: Conformal Invariants. Topics in Geometric Function Theory. McGraw-Hill, NY (1973)
2. Ahlfors, L.: Lectures on Quasiconformal Mappings, 2nd ed. AMS, Providence (2006)
3. Andreev, F., Kitaev, A.: Transformations $RS_4^2(3)$ of ranks $\leq 4$ and algebraic solutions of the sixth Painlevé equation. Commun. Math. Phys. **228**, 151–176 (2002)
4. Benedetto, R., Goldman, W.: The topology of relative character varieties of a quadruply-punctured sphere. Exp. Math. **8**(1), 85–103 (1999)
5. Boalch, P.: From Klein to Painlevé via Fourier, Laplace and Jimbo. Proc. Lond. Math. Soc. **90**(1), 167–208 (2005)
6. Chen, Z.J., Kuo, T.J., Lin, C.S.: Unitary monodromy implies smoothness along the real axis for some Painleve VI. J. Geom. Phys. **116**, 52–63 (2017)

7. Chen, Z.J., Kuo, T.J., Lin, C.S., Wang, C.L.: Green function, Painlevé VI equation, and Eisenstein series of weight one. J. Diff. Geom. Preprint. http://www.math.ntu.edu.tw/~dragon/Research%20papers/Green-Hecke-final+figure.pdf
8. Desideri, L.: Problème de Plateau, équations fuchsiennes et problème de Riemann–Hilbert. Mem. Soc. Math. Fr. **133**, vi+116 (2013)
9. Dubrovin, B.: Painlevé Transcendents in Two-Dimensional Topological Field Theory, The Painlevé Property, 287–412, CRM Series on Mathematical Physics. Springer, New York (1999)
10. Eremenko, A., Gabrielov, A.: Rational functions with real critical points and the B. and M. Shapiro conjecture in real algebraic geometry. Ann. Math. **155**, 105–129 (2002)
11. Eremenko, A., Gabrielov, A.: Spherical rectangles. Arnold Math. J. **2**(4), 463–486 (2016)
12. Eremenko, A., Gabrielov, A.: On metrics of curvature 1 with four conic singularities on tori and on the sphere. Ill. J. Math. arXiv:1508.06510
13. Eremenko, A., Gabrielov, A., Hinkkanen, A.: Exceptional solutions of the Painlevé VI equation. J. Math. Phys. **58**(1), 012701 (2017)
14. Eremenko, A., Gabrielov, A., Shapiro, M., Vainshtein, A.: Rational functions and real Schubert calculus. Proc. AMS **134**(4), 949–957 (2006)
15. Eremenko, A., Gabrielov, A., Tarasov, V.: Metrics with four conic singularities and spherical quadrilaterals. Conform. Geom. Dyn. **20**, 28–175 (2016)
16. Eremenko, A., Gabrielov, A., Tarasov, V.: Spherical quadrilaterals with three non-integer angles. J. Math. Phys. Anal. Geom. **12**(2), 134–167 (2016)
17. Fricke, R., Klein, F.: Vorlesungen über die Theorie der automorphen Funktionen, 1-er Band. Teubner, Leipzig (1897)
18. Fuchs, R.: Sur les équations différentielles linéaires du second ordre. C. R. **141**, 555–558 (1905)
19. Gambier, B.: Sur les équations différentielles du second ordre et du premier degré dont l'intégrale générale est a points critiques fixes. Acta Math. **33**, 1–55 (1909)
20. Golubev, V.: Vorlesungen über Differentialgleichungen im Komplexen. VEB Deutscher Verlag der Wissenschaften, Berlin (1958)
21. Goluzin, G.: Geometric Theory of Functions of a Complex Variable. AMS, Providence (1969)
22. Gromak, V., Laine, I., Shimomura, S.: Painlevé Differential Equations in the Complex Plane. Walter de Gruyter & Co., Berlin (2002)
23. Guzzetti, D.: A review of the sixth Painlevé equation. Constr. Approx. **41**(3), 495–527 (2015)
24. Hitchin, N.: Twistor spaces, Einstein metrics and isomonodromic deformations. J. Diff. Geom. **42**(1), 30–112 (1995)
25. Horowitz, R.: Characters of free groups represented in the two-dimensional special linear group. Commun. Pure Appl. Math. **25**, 635–649 (1972)
26. Hurwitz, A., Courant, R.: mit einem Anhang von Röhrl, Allgemeine Funktionentheorie und eliptische Funktionen, vierte vermeherte und verbesserte Auflage. Springer, Berlin (1964)
27. Ihlenburg, W.: Über die geometrischen Eigenschaften der Kreisbopgenvierecke. Nova Acta Leopoldina **92**, 1–79 (1909)
28. Inaba, M., Iwasaki, K., Saito, M.-H.: Bäcklund transformations of the sixth Painlevé equation in terms of the Riemann-Hilbert correspondence. IMRN **1**, 1–30 (2004)
29. Iwasaki, K.: An area preserving action of the modular group on cubic surfaces and Painlevé VI equation. Commun. Math. Phys. **242**, 185–219 (2003)
30. Jimbo, M.: Monodromy problem and the boundary condition for some Painlevé equations. Publ. Res. Inst. Math. Sci. **18**(3), 1137–1161 (1982)
31. Klein, F.: Über die Nullstellen der hypergeometrischen Reihe. Math. Ann. **37**, 573–590 (1890)
32. Kontsevich, M., Manin, Y.: Gromov–Witten classes, quantum cohomology, and enumerative geometry. Commun. Math. Phys. **164**(3), 525–562 (1994)
33. Lisovyy, O., Tykhyy, Y.: Algebraic solutions of the sixth Painlevé equation. J. Geom. Phys. **85**, 124–163 (2014)
34. Litvinov, A., Lukyanov, S., Nekrasov, N.: Classical conformal blocks and Painlevé VI. J. High Energy Phys. **7**, 1–19 (2014)
35. Mazzocco, M.: Picard and Chazy solutions to the Painlevé VI equation. Math. Ann. **321**(1), 157–195 (2001)
36. Morgan, J., Shalen, P.: Valuations, trees, and degenerations of hyperbolic structures, I. Ann. Math. **120**(3), 401–476 (1984)
37. Okamoto, K.: Studies in Painlevé equations I. Sixth Painlevé equation PVI. Ann. Mat. Pura Appl. **146**(4), 337–381 (1987)
38. Okamoto, K.: On the $\tau$-function of the Painlevé equations. Physica **2D**, 525–535 (1981)
39. Painlevé, P.: Sur les équations différentielles du second ordre et d'ordre supérieur dont l'intégrale générale est uniforme. Acta Math. **25**, 1–85 (1901)
40. Picard, E.: Mémoire sur la théorie des fonctions algébriques de deux variables. J. Math. **5**, 135–319 (1889)

41. Sasaki, T., Yoshida, M.: A geometric study of the hypergeometric function with imaginary exponents. Exp. Math. **10**(3), 321–330 (2001)
42. Schilling, F.: Ueber die Theorie der symmetryschen S-Funktionen mit einem einfachen Nebenpunkte. Math. Ann. **51**, 481–522 (1899)
43. Van Vleck, E.: On certain differential equations of the second order allied to Hermite's equation. Am. J. Math. **21**, 126–167 (1899)
44. Van Vleck, E.: A determination of the number of real and imaginary roots of the hypergeometric series. TAMS **3**(1), 110–131 (1902)
45. Watanabe, H.: Birational canonical transformations and classical solutions of the sixth Painlevé equation. Ann. Scuola Norm. Sup. Pisa Cl. Sci. (4) **27**(3–4), 379–425 (1998)

Communicated by P. Deift